UNITED NATIONS EDUCATIONAL, SCIENTIFIC AND CULTURAL ORGANIZATION
INTERNATIONAL ATOMIC ENERGY AGENCY
INTERNATIONAL CENTRE FOR THEORETICAL PHYSICS

SMR/917 - 21

SECOND WORKSHOP ON SCIENCE AND TECHNOLOGY OF THIN FILMS

(11 - 29 March 1996)

" Fabrication of quantum wells and superlattices by molecular beam epitaxy." (PART II)

presented by:

R. HEY
Paul Drude Institut für Festkörperelektronik
Hausvogteiplatz 5-7
10117 Berlin
Germany

AFM image

of a GaAs surface after thermal oxide desorption

10 µm x 10 µm, gray scale 16 nm —[110]→

RHEED patterns

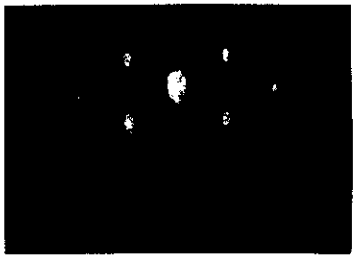

$[1\bar{1}0]$

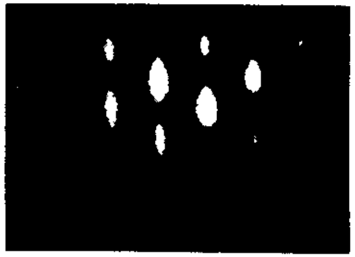

[110]

RHEED patterns

of the growing surface *and* during growth interruption

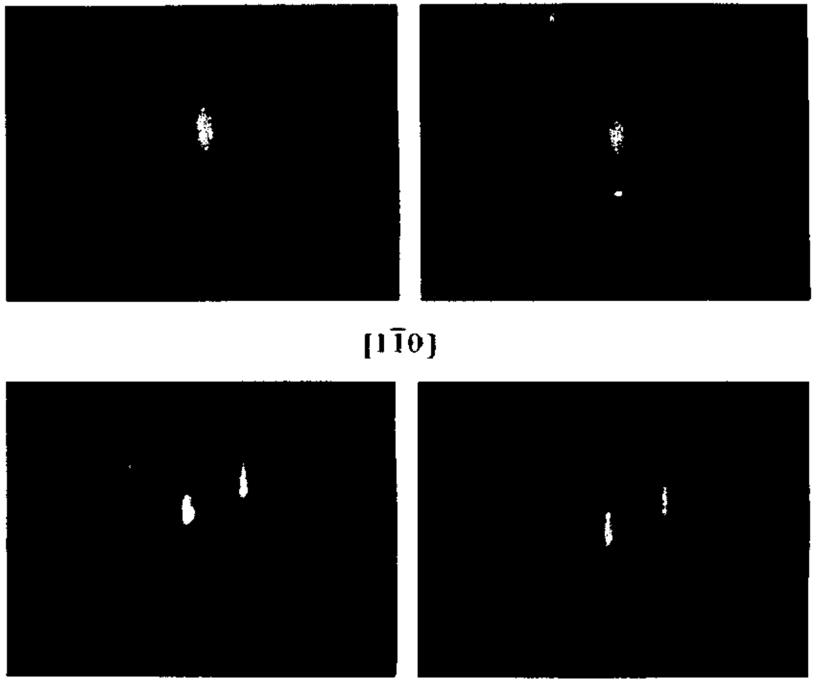

$[1\bar{1}0]$

[110]

(3x1) (2x4)

AFM image of the singular (001)GaAs surface

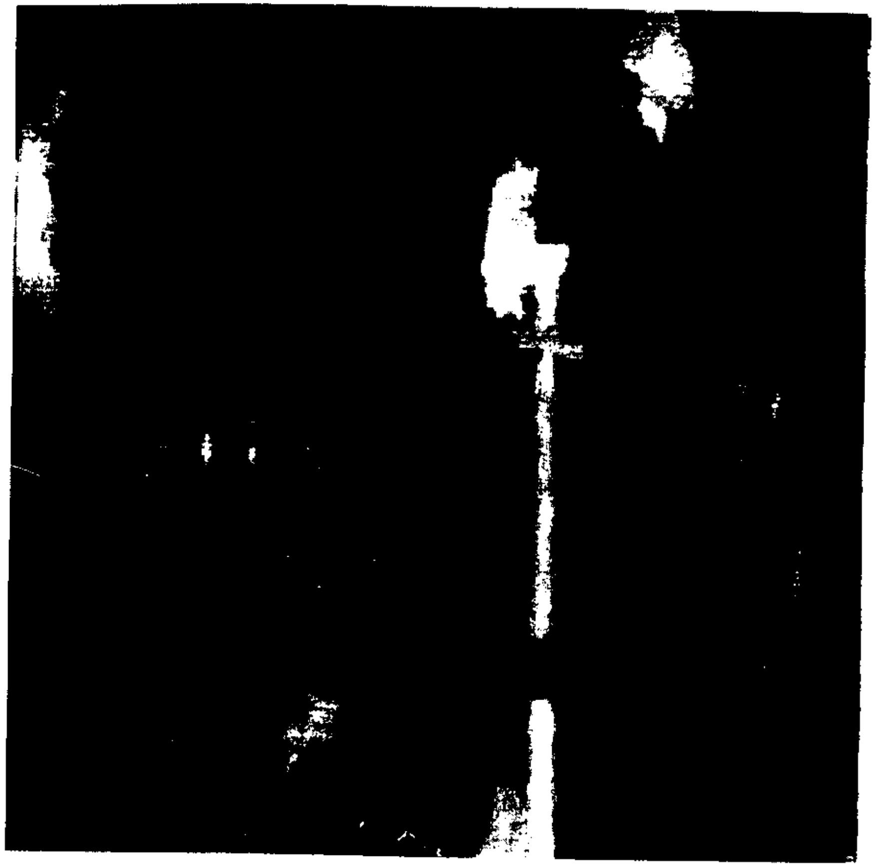

5 µm x 5 µm,   d = 120 nm   — [110]→

AFM images of GaAs epilayer surfaces

miscut towards (111)Ga (a) and (1$\bar{1}$1)As (b): α ≈ 0.08°

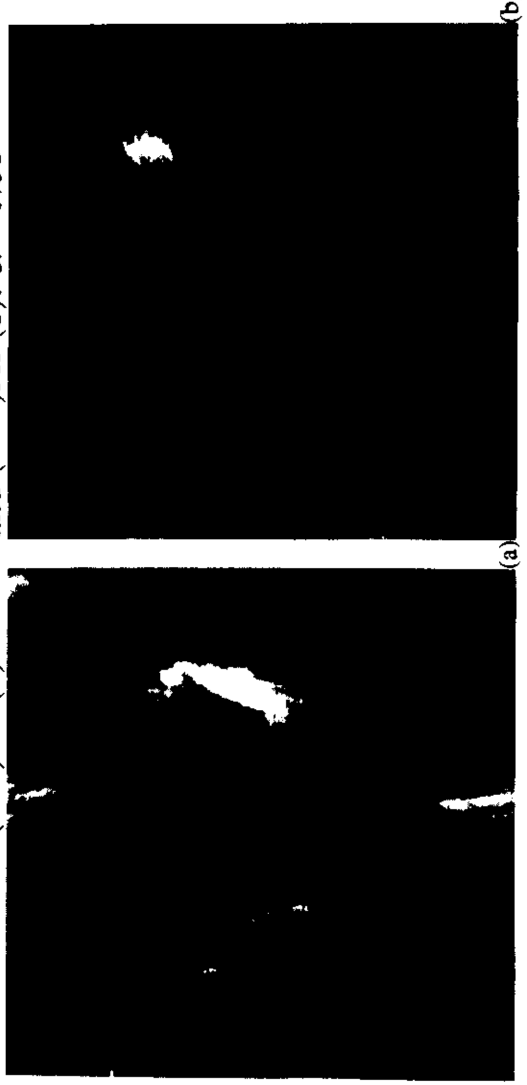

5 µm x 5 µm ,   d = 120 nm,   gray scale 3 nm —[110]→

Ga-terminated step-edges   As-terminated step-edges

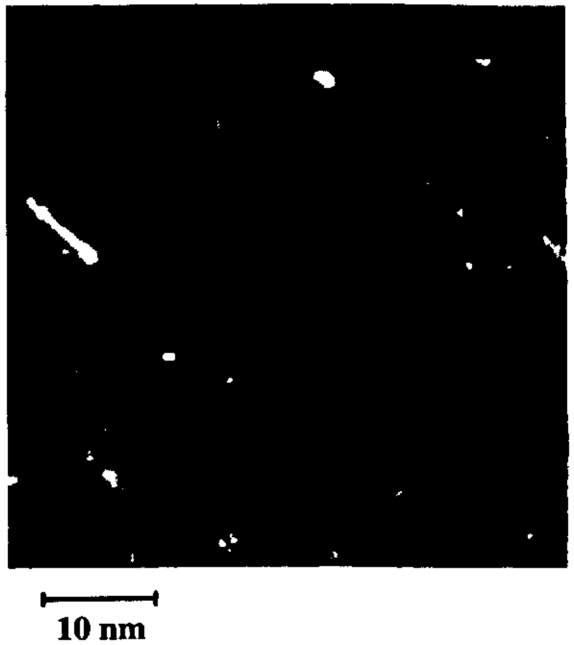

STM image of a

B-step system on

GaAs(001)

0.5°

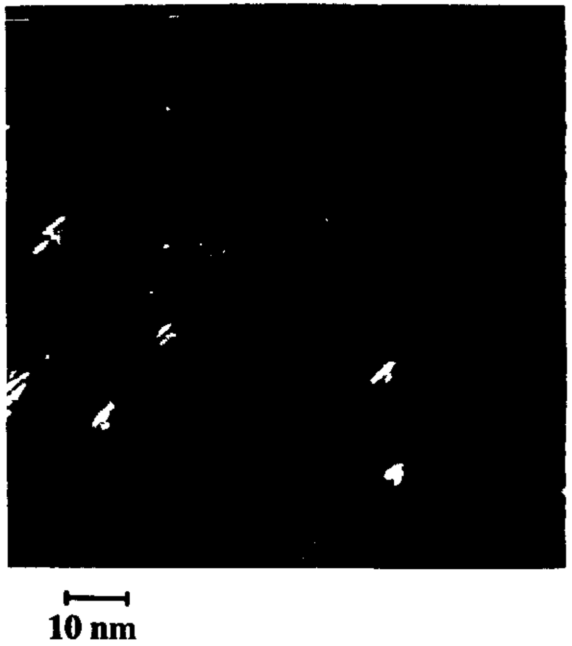

STM image of a

A-step system on

GaAs(001)

0.5 °

AFM image of a vicinal GaAs(001) surface near the vortex

15 µm x 15 µm d = 120 nm gray scale 3 nm —[110]→

inclination towards (111)Ga increases from the left to the right side

AFM images of misoriented GaAs(001) surfaces

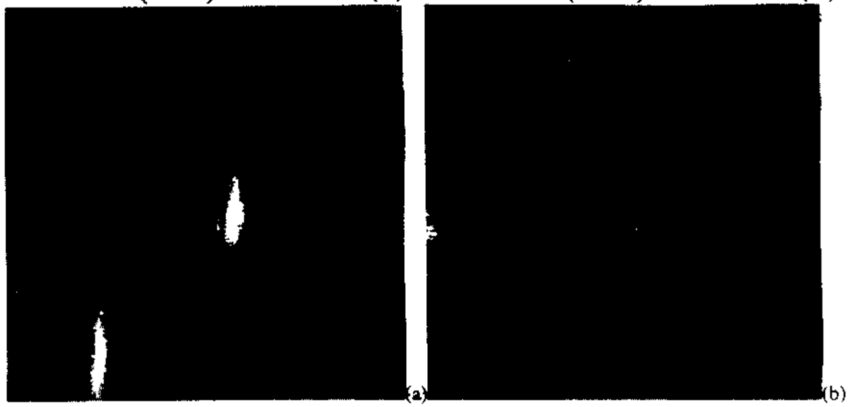

towards (111)Ga $\alpha \approx 1°$ (a) towards $(1\bar{1}1)$As $\alpha \approx 2°$ (b)

5 µm x 5 µm d = 120 nm gray scale 6 nm

— [110]→ — $[1\bar{1}0]$→

towards $(1\bar{1}1)$As $\alpha \approx$4-5°

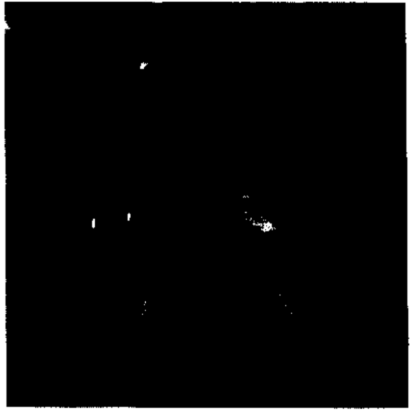

gray scale 100 nm

AFM images of vicinal GaAs(001) surfaces

on unintentionally misoriented wafers $\alpha \approx 0.09°$

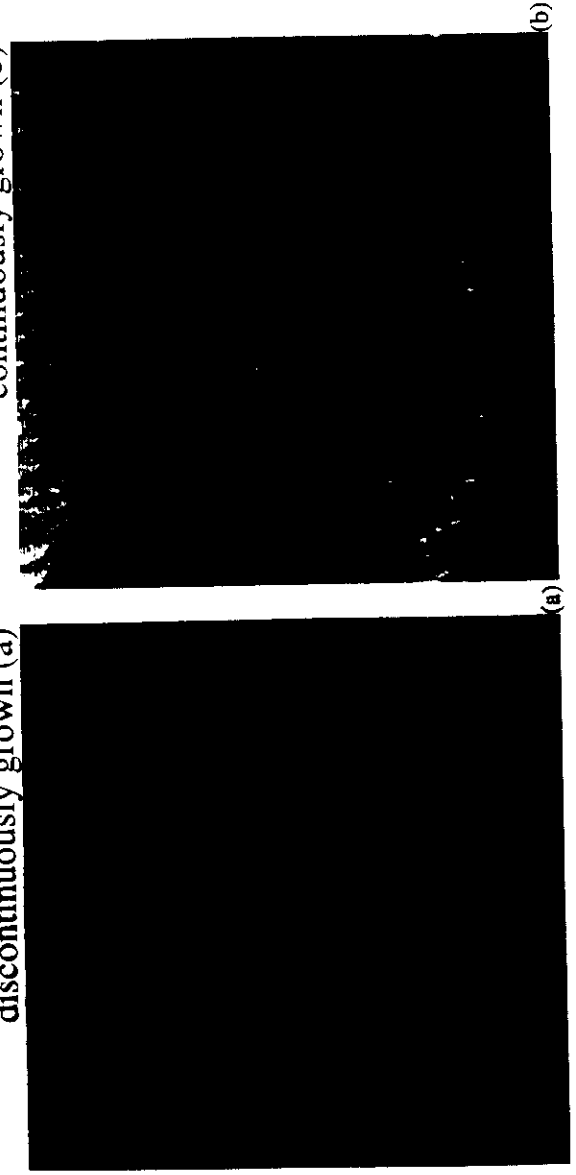

continuously grown (b)

discontinuously grown (a)

5 µm x 5 µm d = 120 nm gray scale 2 nm — <110> →

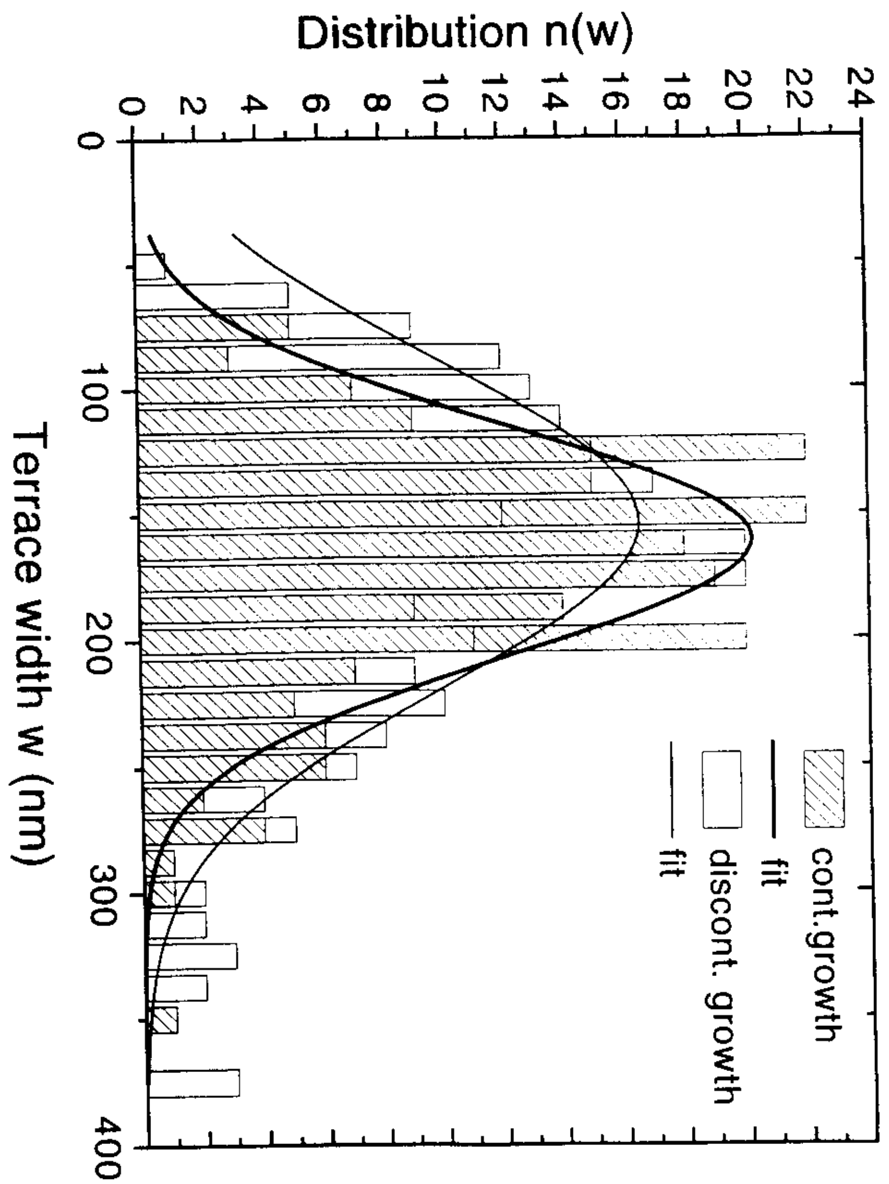

GaAs(001): Step bunching after annealing at growth temperature

T_s= 600°C; BEP = 24; v = 0.145μm/h; (3x1): d = 200nm ; $\alpha \approx 0.2°$

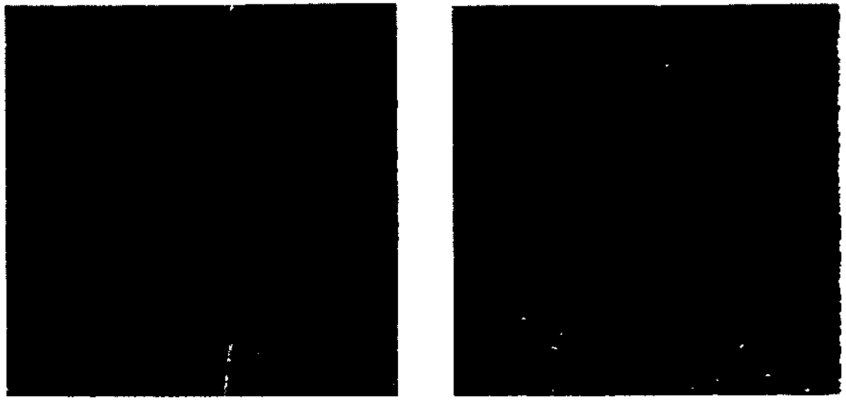

#411 ***0 min*** anneal 3μm x 3μm

#419 ***2 min*** anneal 3μm x 3μm

#417 ***5 min*** anneal 3μm x 3μm

#415 ***20 min*** anneal 3μm x 3μm

Summary : homoepitaxial growth

singular GaAs(001) surface

- ***growth instability*** with respect to regular island shape and step edge profile; selfsimilarity
- ***Ga migration length*** only about 100 nm (island separation)

vicinal GaAs(001) surfaces with $0.1° \leq \alpha \leq 0.2°$

- highly ***regular step systems***
- common ***lateral roughness*** on a ***µm-scale*** irrespective of crystal material and its misorientation
- ***anisotropic 2-dimensional step bunching***;
  „A-surface": $L_{[1\bar{1}0]} > L_{[110]}$; $L = f(\alpha)$
  „B-surface": rougher, faceting
- ***narrower*** terrace width distributions for ***continuous growth***
- ***annealing*** at T_{growth} strongly affects the initial step array
- ***localized excitons*** due to interface roughness (step-bunches)

Recommendation for obtaining a regular step system:

- mixed step system, but composed of predominantly A-steps
- mean terrace width lower than 150 nm
- continuous growth
- no extended annealing at T_{growth}

Commonly discussed models for the GaAs (2x4) surface reconstruction

As atoms
Ga atoms
dimerized As atoms

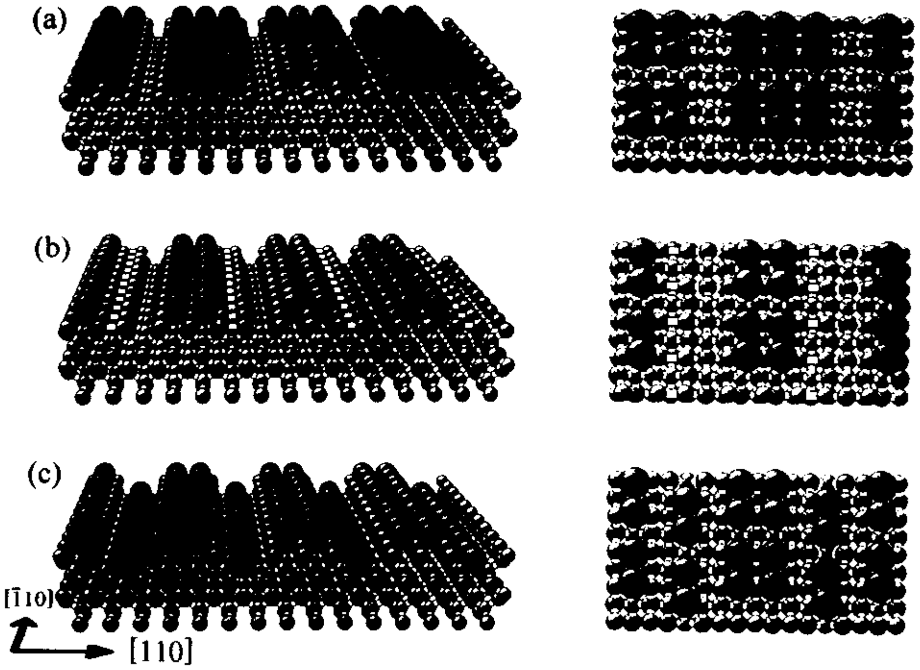

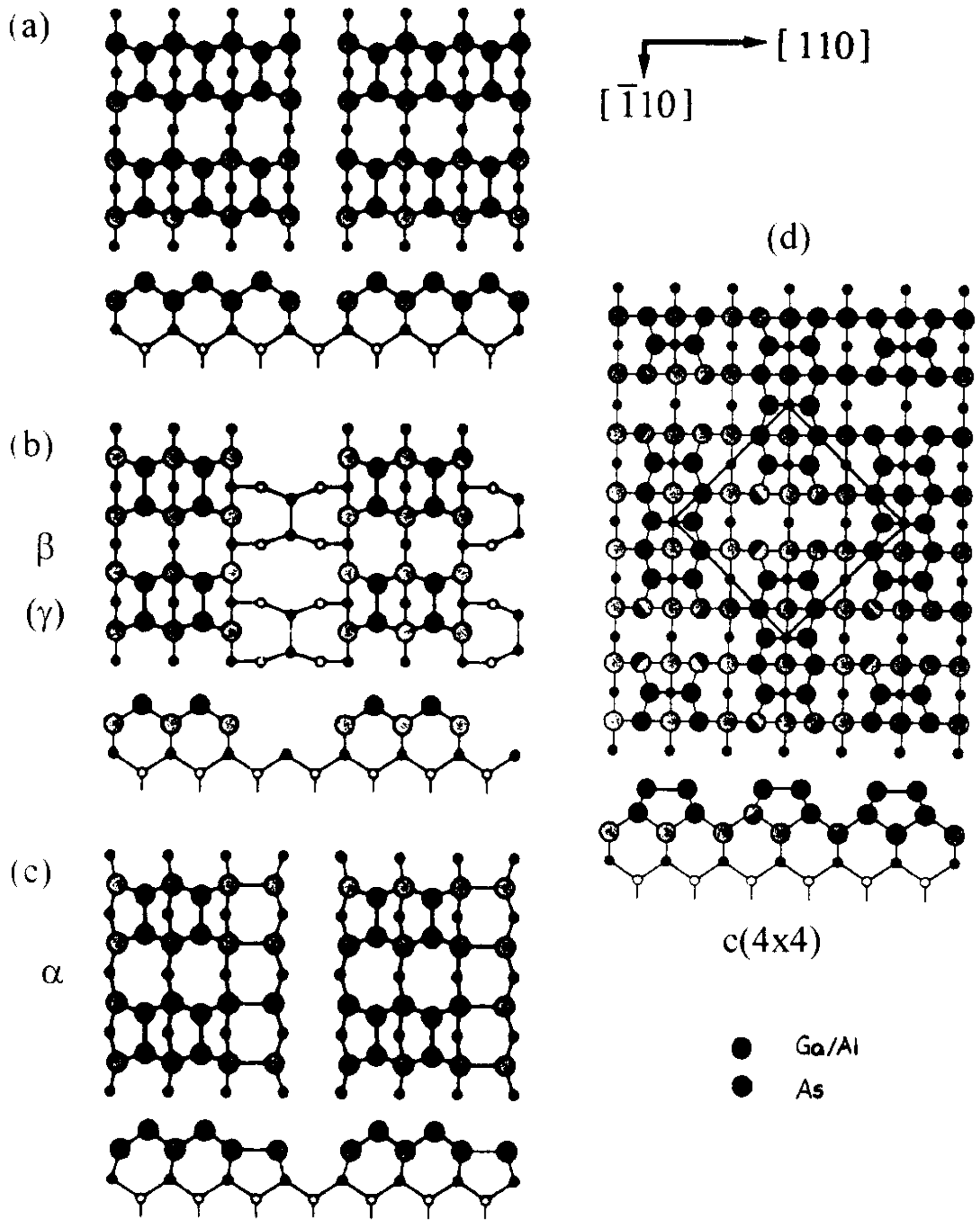

Influence of kinks in the dimer rows

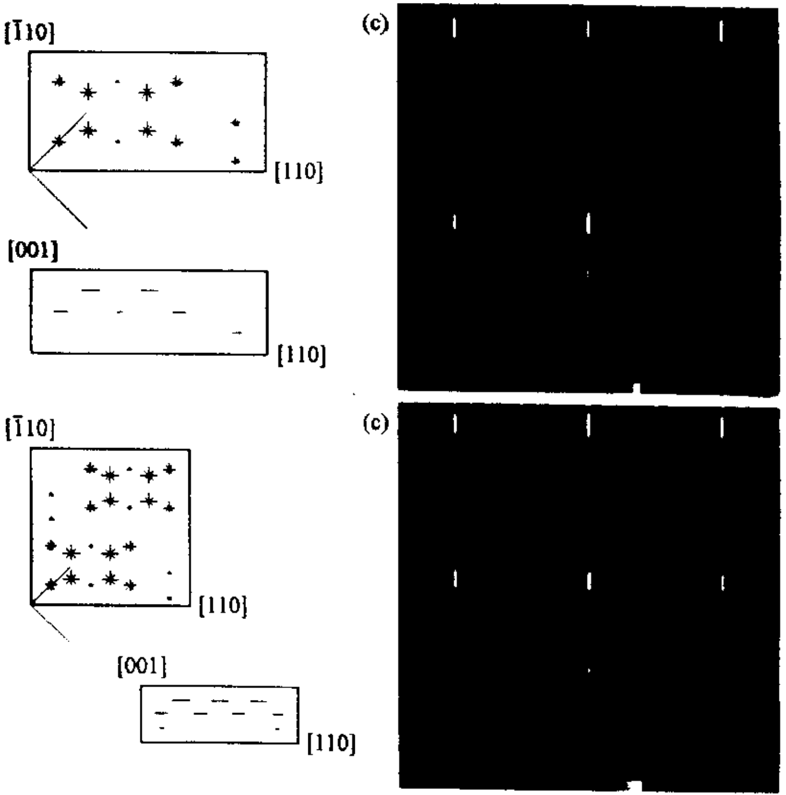

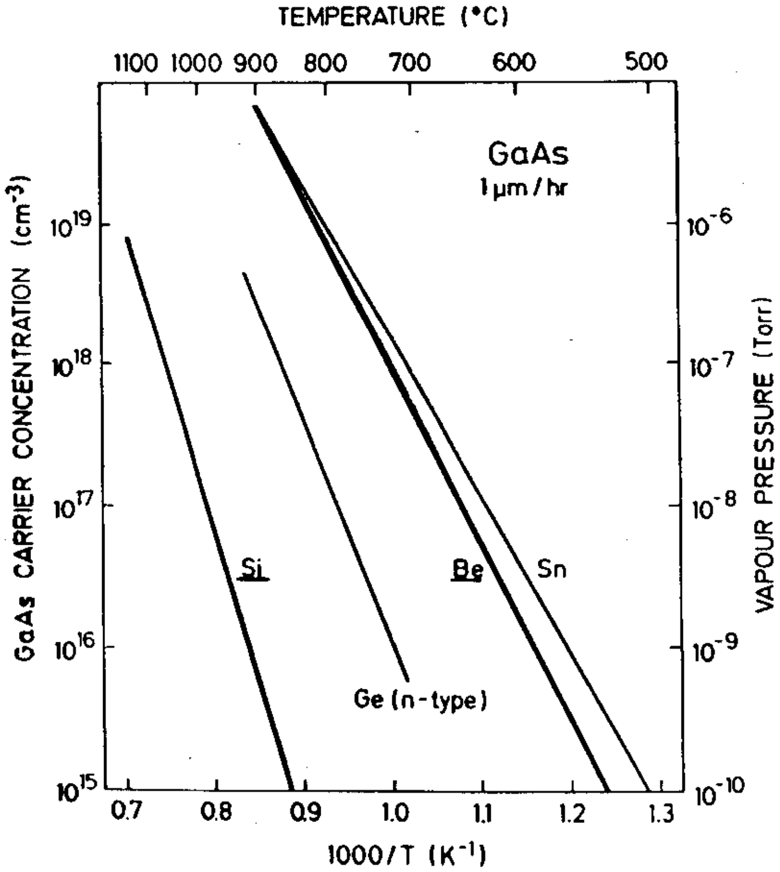

Si deposition and reconstruction evolution

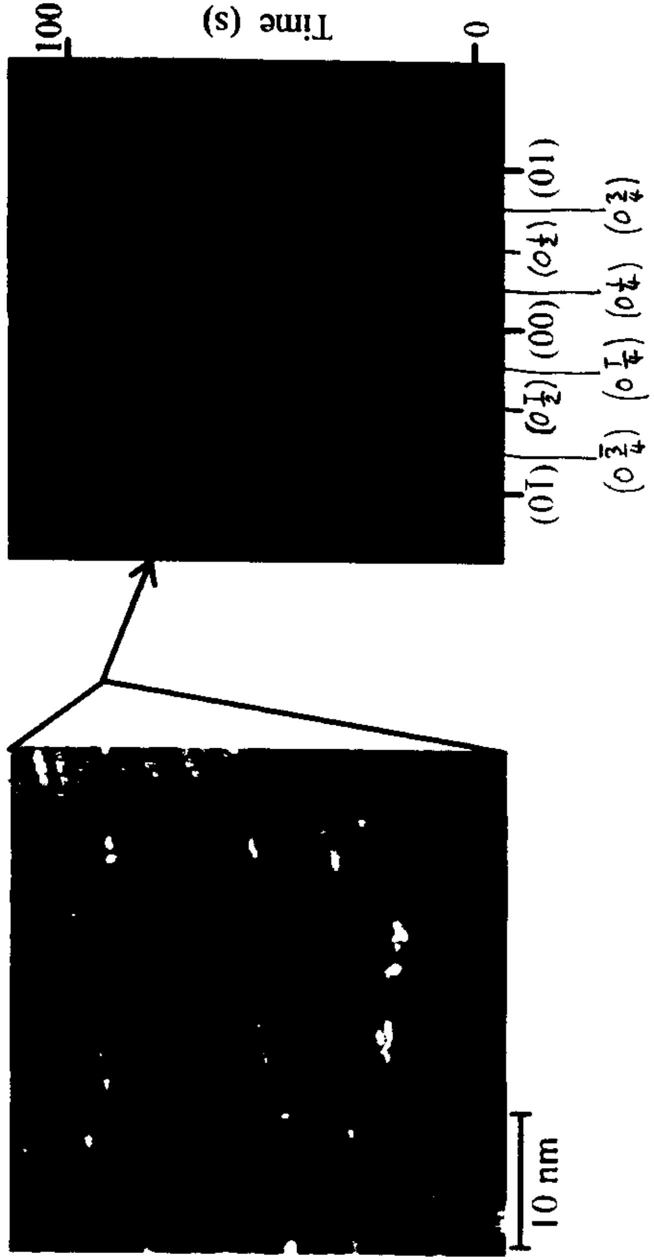

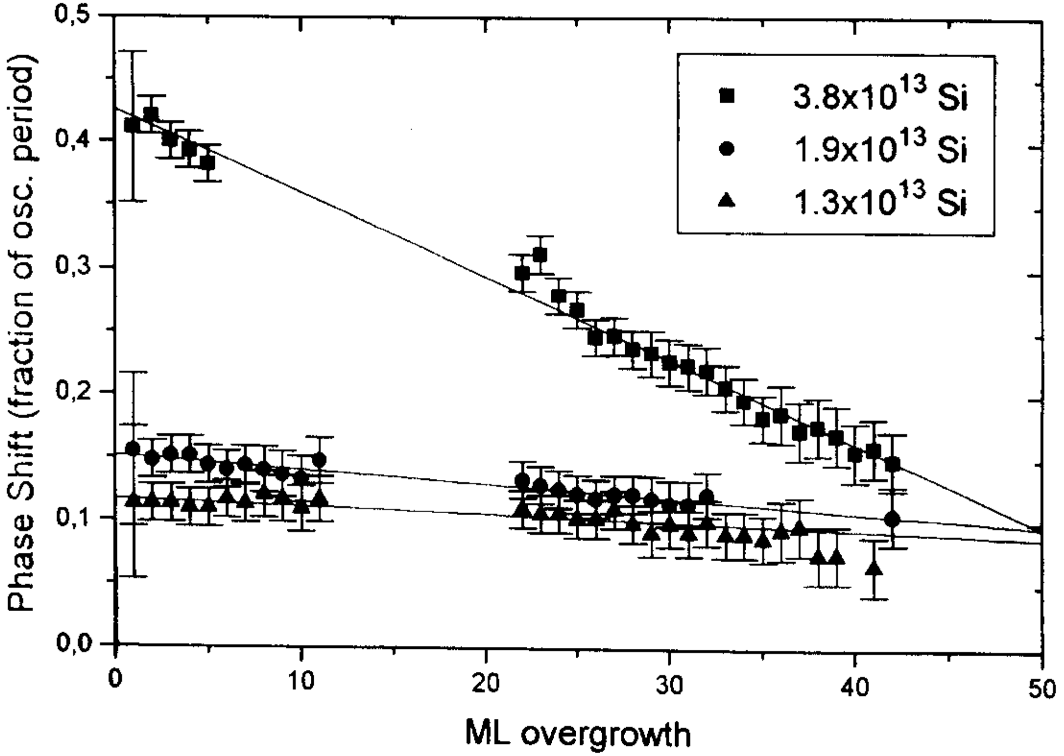

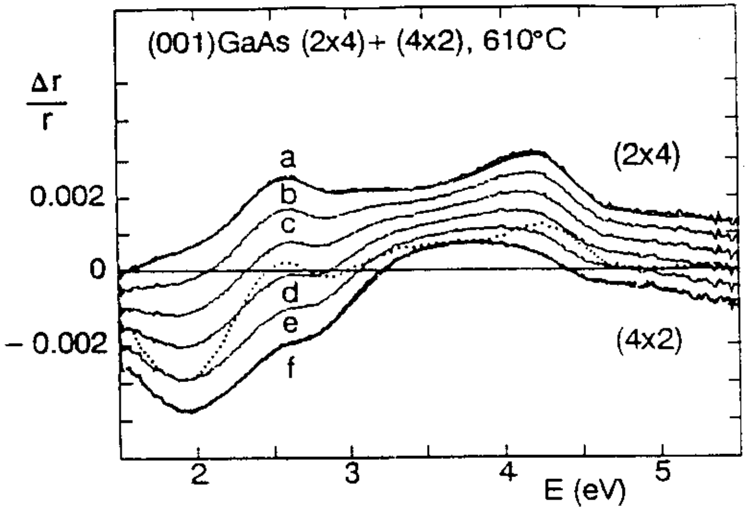

FIG. 9. RD spectra synthesized from linear combinations of (2×4) and (4×2) spectra at 610°C

I. Kamiya, D.E. Aspnes, L. Florez, and J.B. Harbison,
Phys. Rev. B 45 (1992) 15894

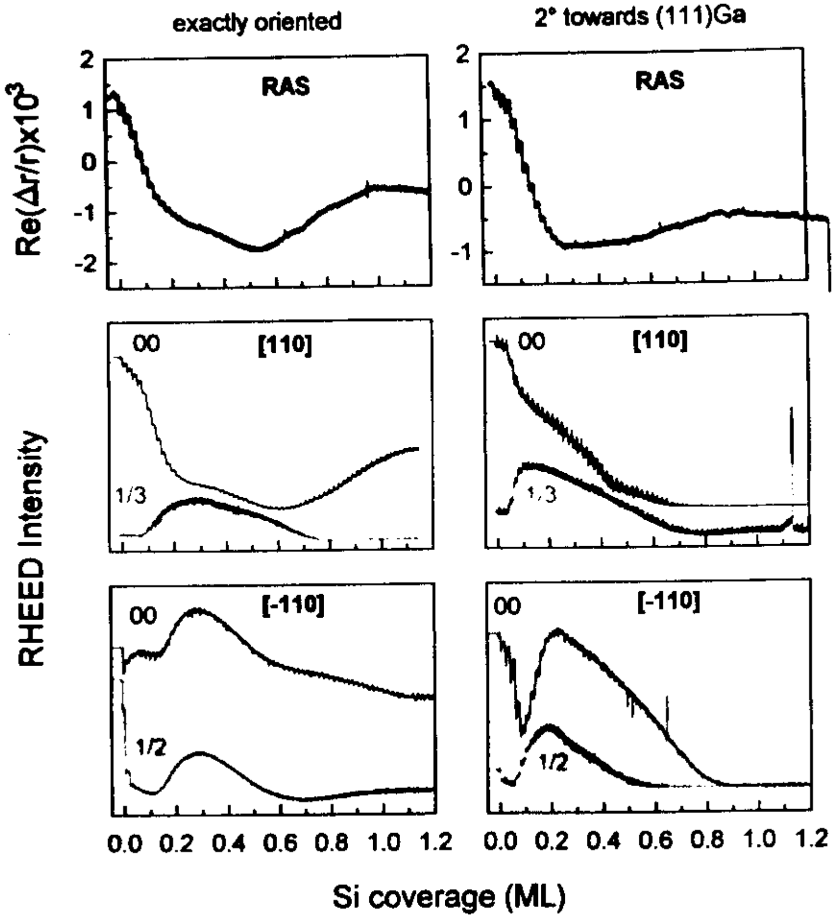

Fig. 6

T_S: 590°C
$p_{BEP}As_4$: 1×10^{-6} Torr
Si flux: 2×10^{11} cm^{-2}s^{-1}
pulse: 60s interruption: 180s

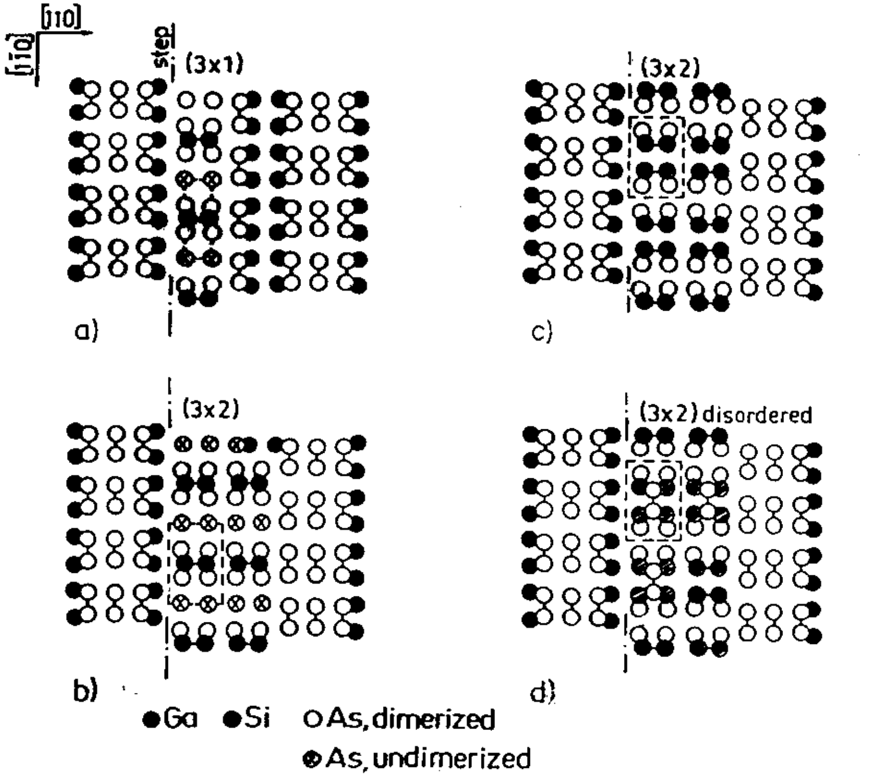

Evolution of the (3 x 2) reconstruction

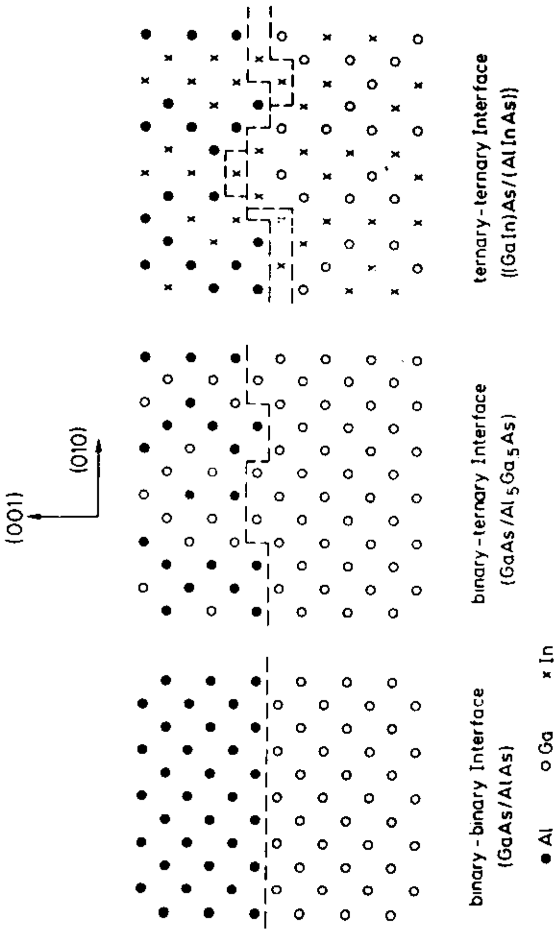

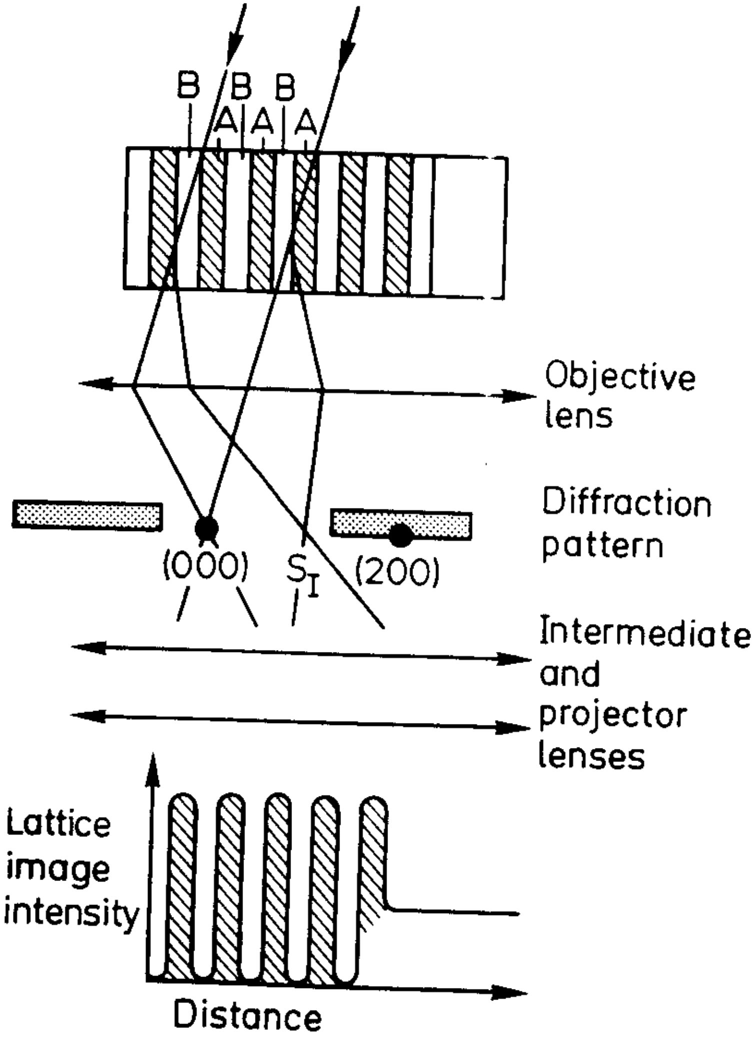

Transmission Electron Diffraction (TED) Pattern

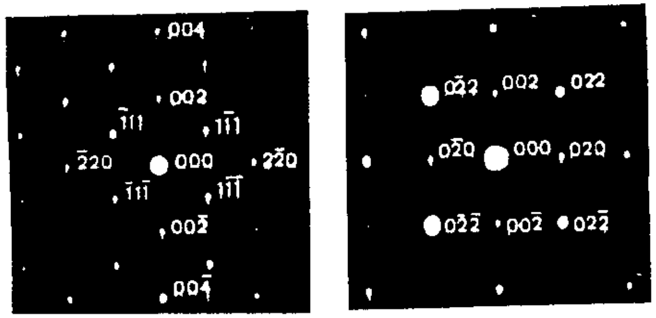

(a) (b)

[110] [100]

e-beam incidence

Construction of lattice image

[110] : Interference between direct (000) beam, four {111} diffracted and two {002} diffracted beams

[100] : Interference between direct (000) beam, four {002} diffracted and four {022} diffracted beams

TEM-Aufnahme der Segregationsstruktur entlang der Hauptachsen der Oberflächenanisotropie

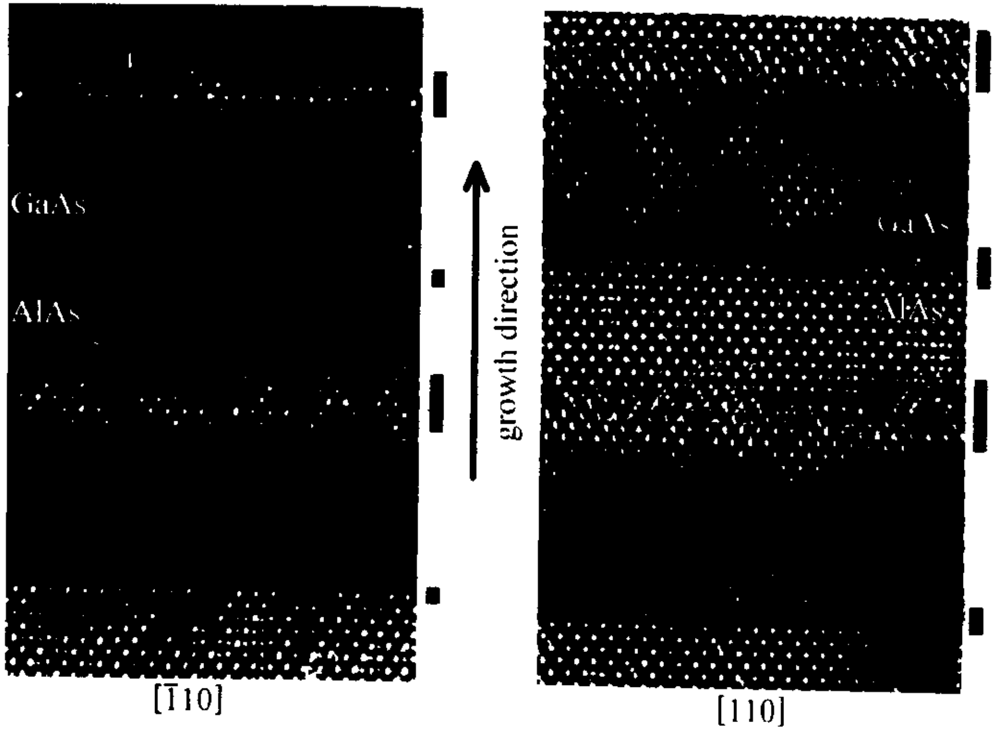

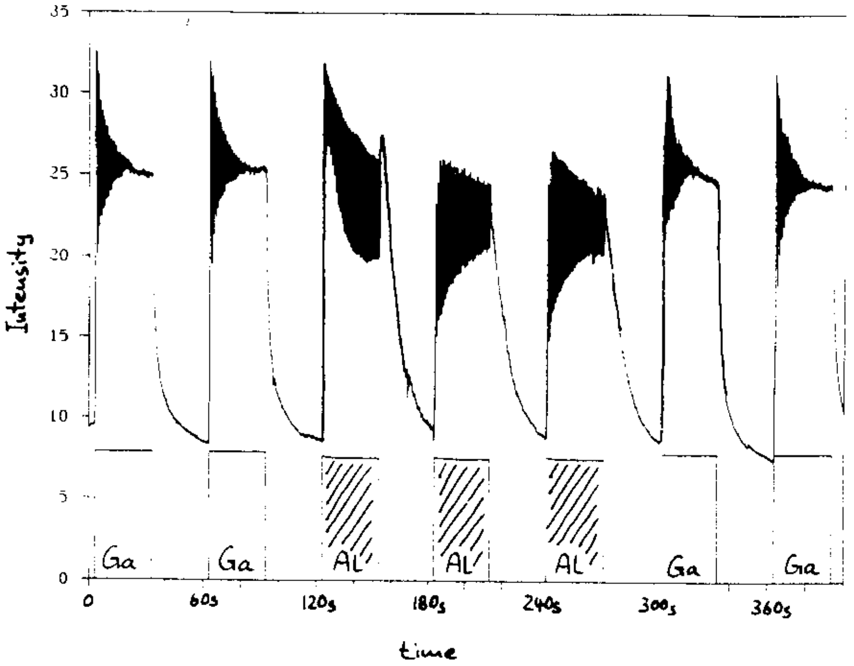

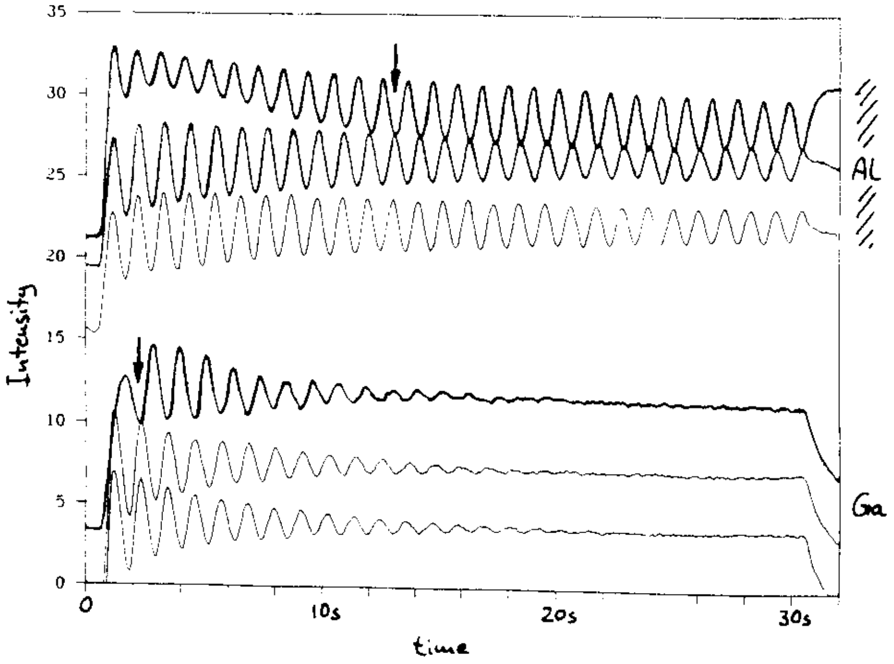

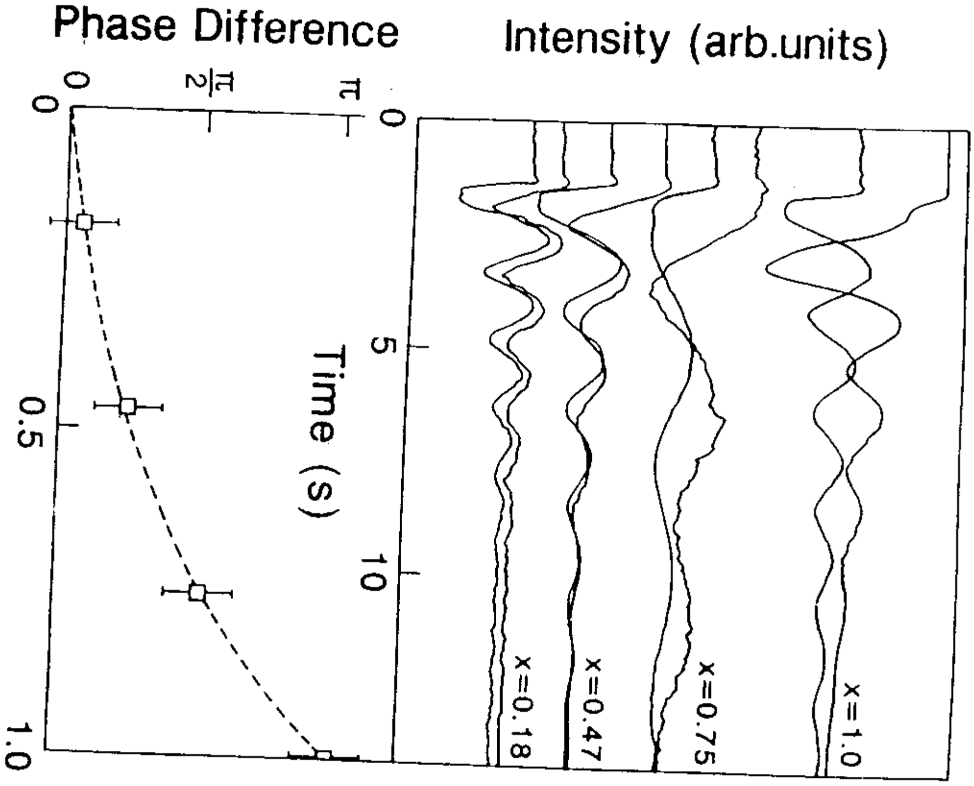

Initial GaAs(001) surface before AlAs deposition

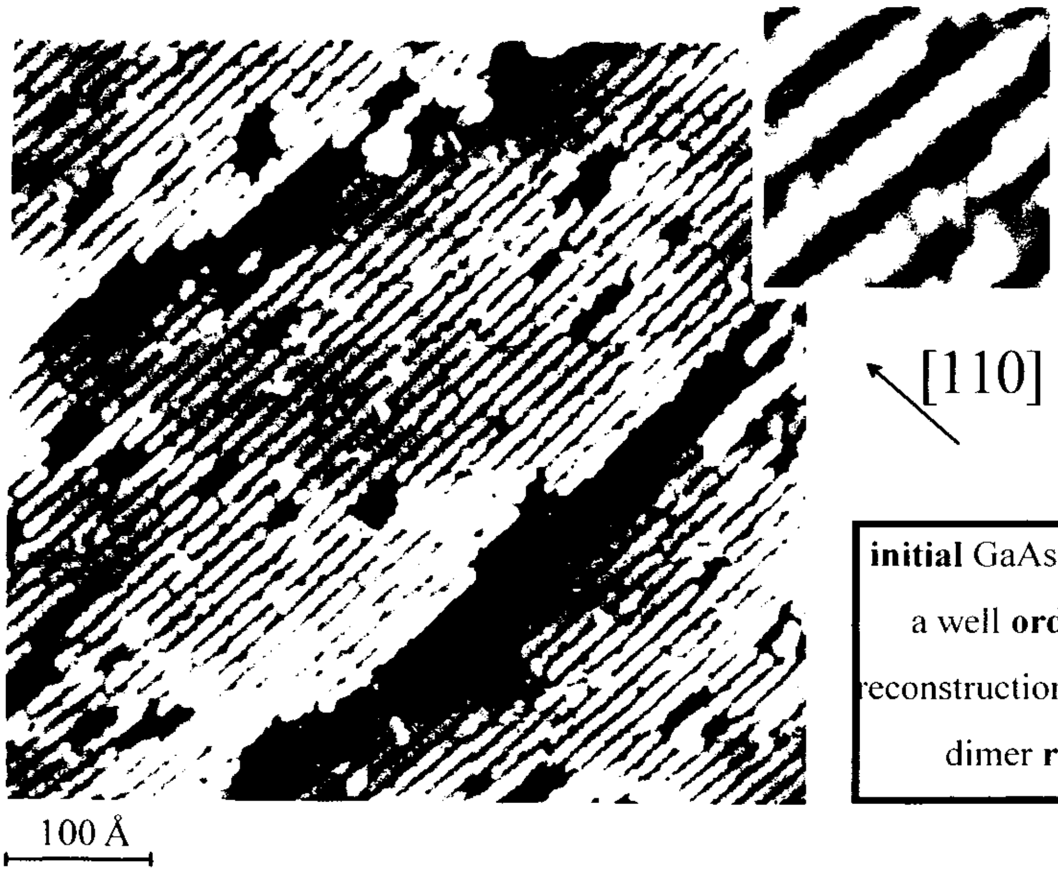

(2x4) unit meshes contain two As dimers and two missing dimers

initial GaAs(001) surface showing a well **ordered** As-rich (2x4) reconstruction with **straight** missing dimer **rows** along [-110]

The normal GaAs/AlAs interface

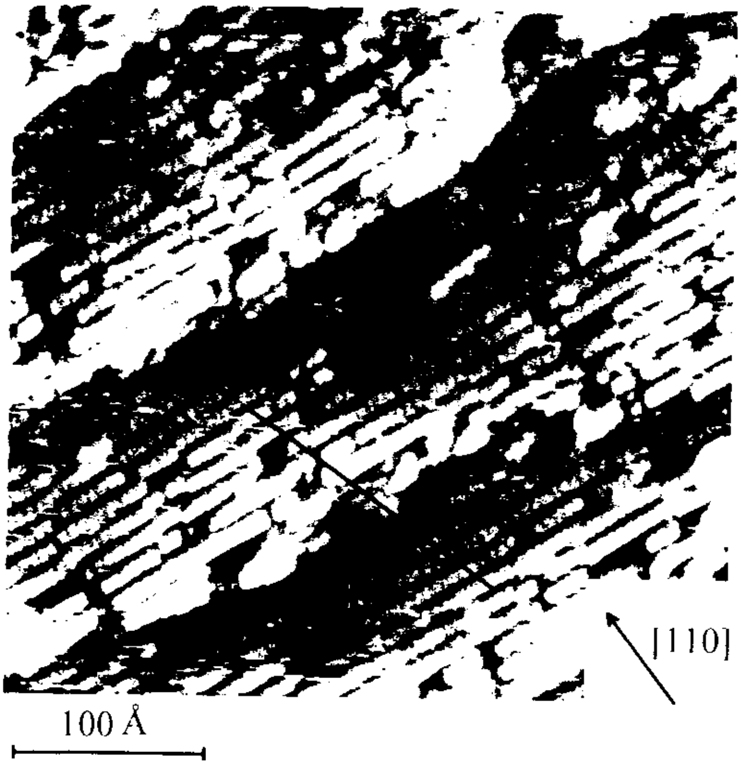

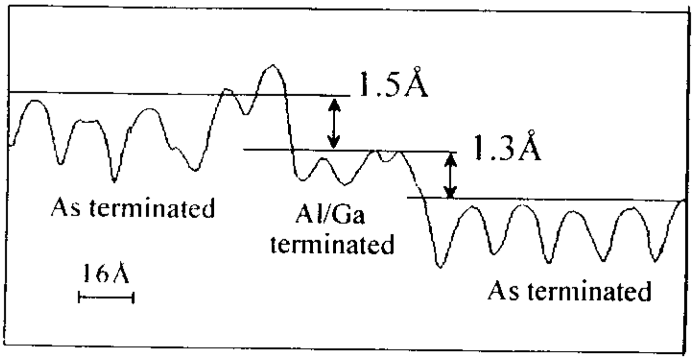

surface after the deposition of
10 ML AlAs on the GaAs buffer

a strong **Ga segregation** leads to a gradual change of the reconstruction

compensating surface defects (**kinks**) appear in the rows of the (2x4) structure

The inverted AlAs/GaAs interface

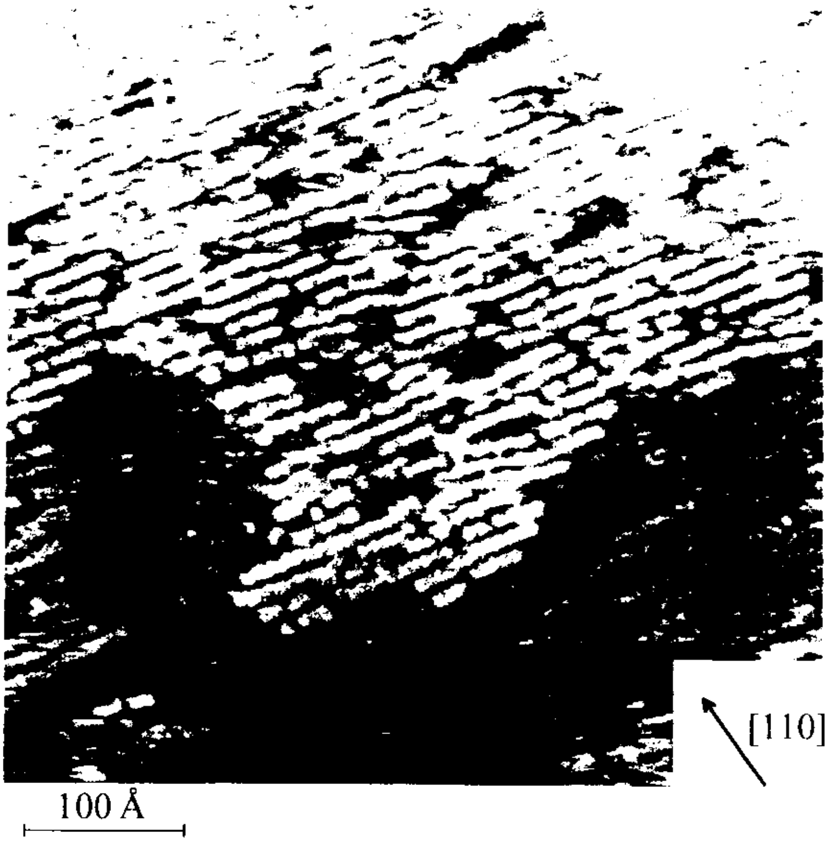

surface after the deposition of
1ML GaAs on 50 ML AlAs

(2x4) reconstruction appears again

high **kink** density indicates a high density of intrinsic point defects **(As vacancies)**

defects are burried at the inverted interface plane during the **abrupt** formation of this interface type

Morphological changes during the interface formation

large scale STM scans of 4000 x 4000 Å^2 in size showing the surface morphology for different stages of the formation of normal and inverted interfaces

morphology appears less drastically changed as expected

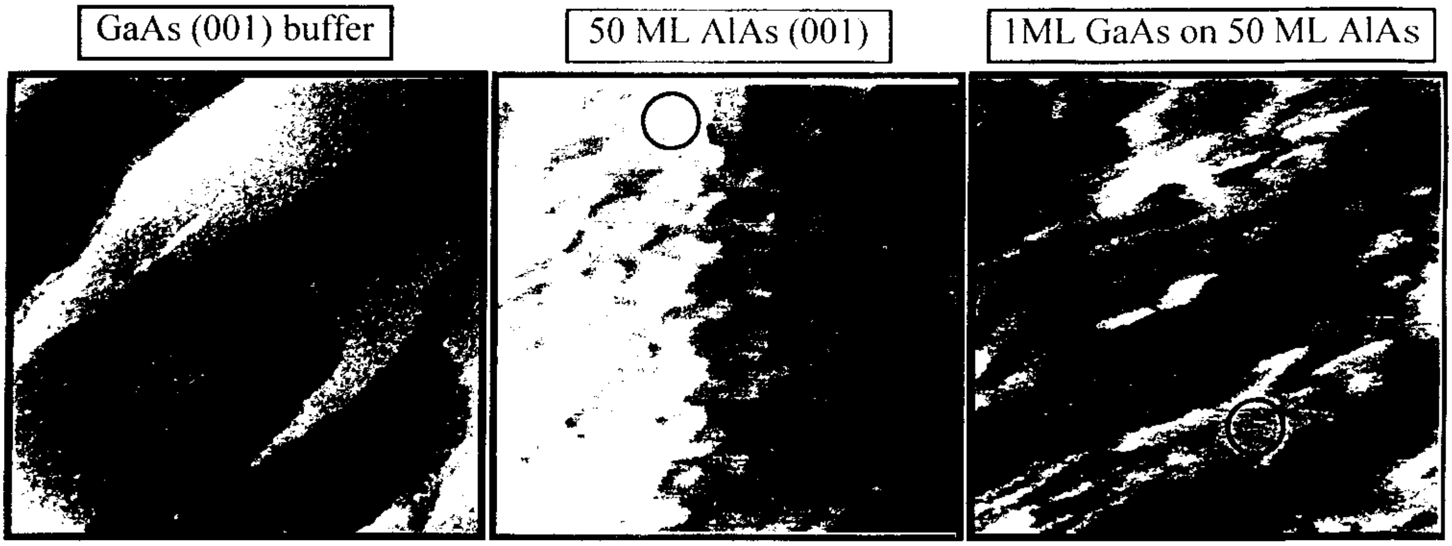

GaAs (001) buffer

50 ML AlAs (001)

1ML GaAs on 50 ML AlAs

○ marks the averaged value of an exciton diameter in GaAs for comparison

---

Summary and conclusions STM

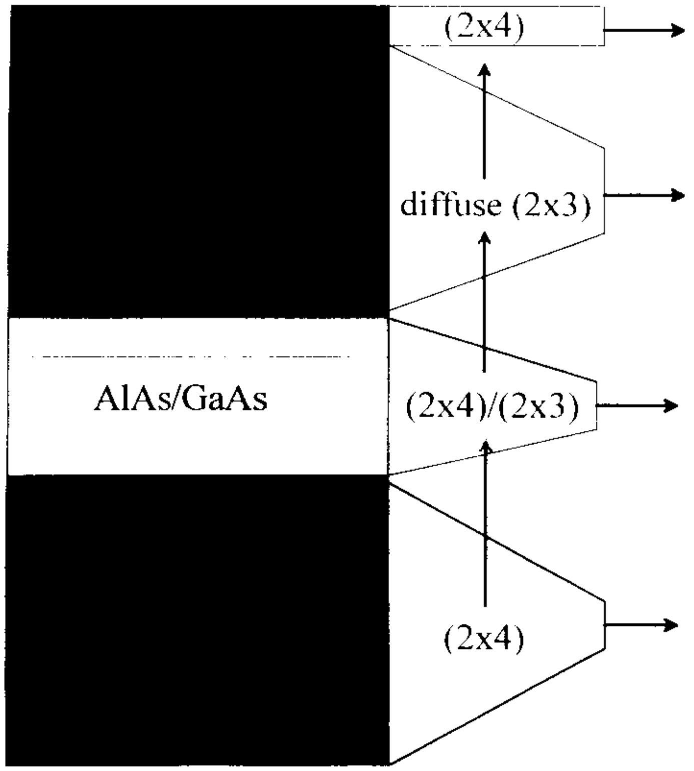

inverted interface:
abrupt reconstruction change (within 1 ML) **defects** (As vacancies) are **burried** at the interface causing a **high kink density** in STM

pure AlAs surface:
intrinsic point defects (As vacancies) remain at the growing AlAs surface **without** being incorporated

normal interface:
continuous reconstruction change (10 ML) due to the Ga segregation, presence of As vacancies inherent to the AlAs growth, numerous **kinks** appear in response to deep electronic states corresponding to the As vacancies

GaAs buffer:
well ordered reconstruction with straight dimer rows, **no** compensating **defects** (kinks) visible

growth direction

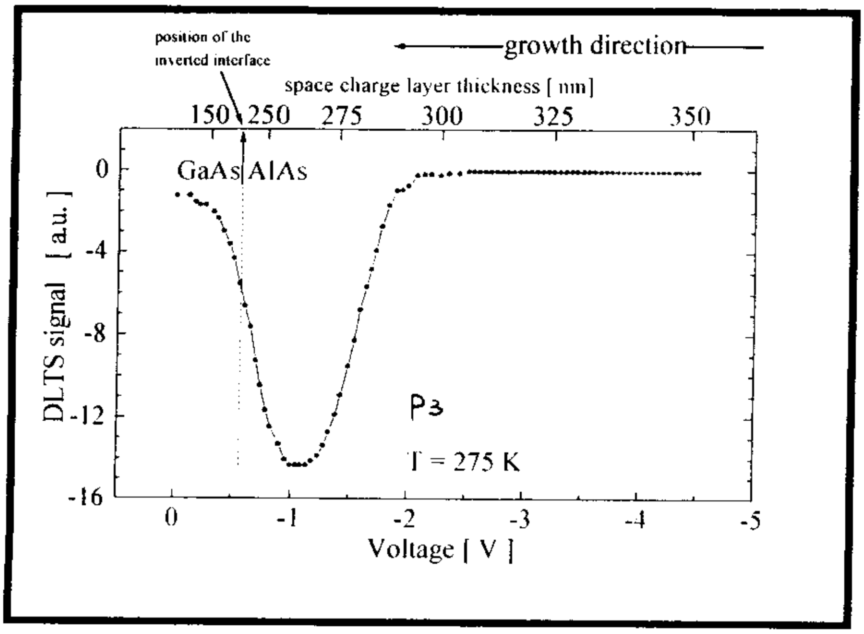

DLTS spectra revealing a high density of **intrinsic point defects** incorporated close to or almost
at the inverted interface plane
identified as negatively charged **As vacancies**

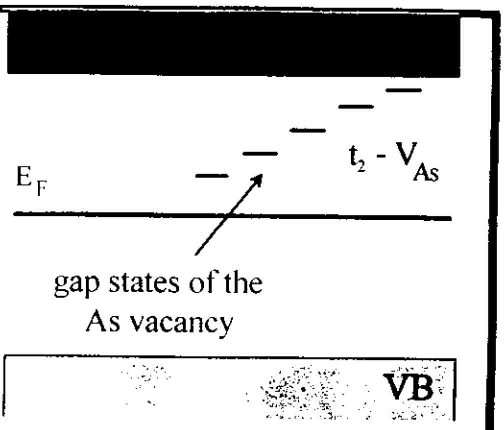

corresponding defect states can **release** up to five **electrons** due to its position above the Fermi level

compensating **kinks** appear in response to these released charges

kinks in STM images are related to the creation of **As vacancies** inherent to the AlAs growth

P2 ··· P6 electron traps in n GaAs / n AlAs

DEPTH PROFILES OF CARRIER CONCENTRATION

$N_{CV} = \frac{2}{A^2 q \varepsilon \varepsilon_0}\left[\frac{\partial 1/C^2}{\partial V}\right]^{-1}$

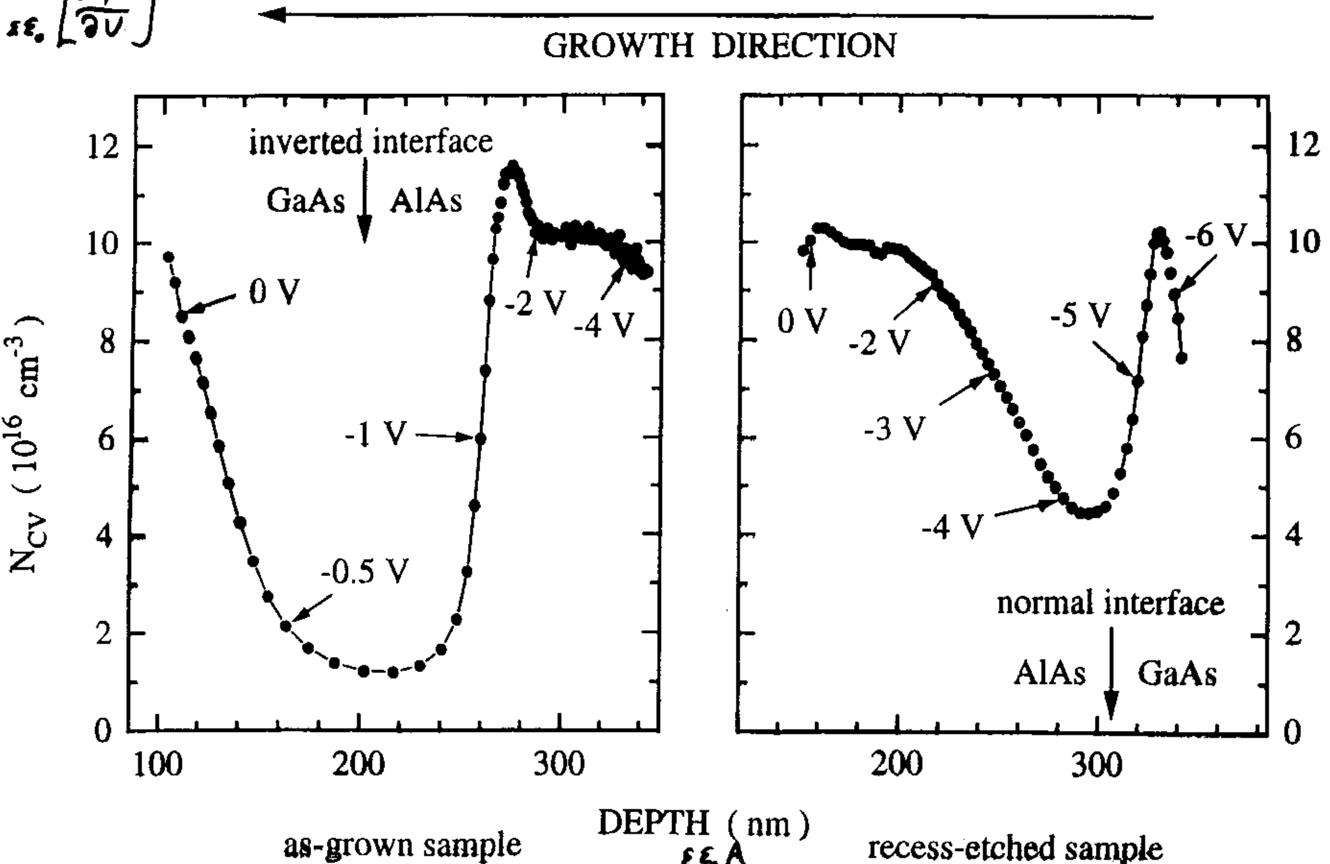

as-grown sample

recess-etched sample

$w = \frac{\varepsilon \varepsilon_0 A}{C}$

DEEP-LEVEL SPECTRA
GaAs/AlAs INTERFACE

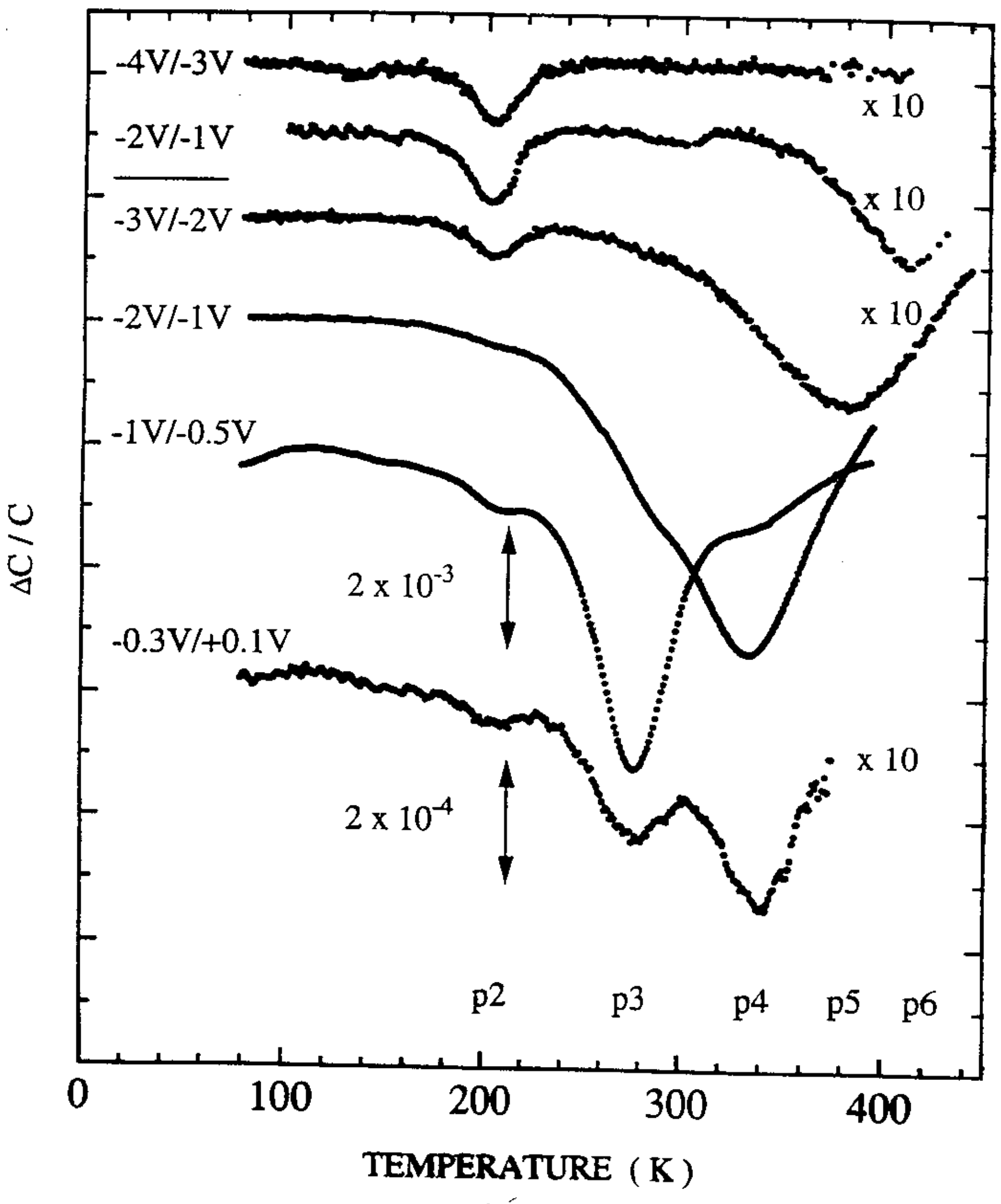

DEPTH PROFILES OF DEEP LEVELS

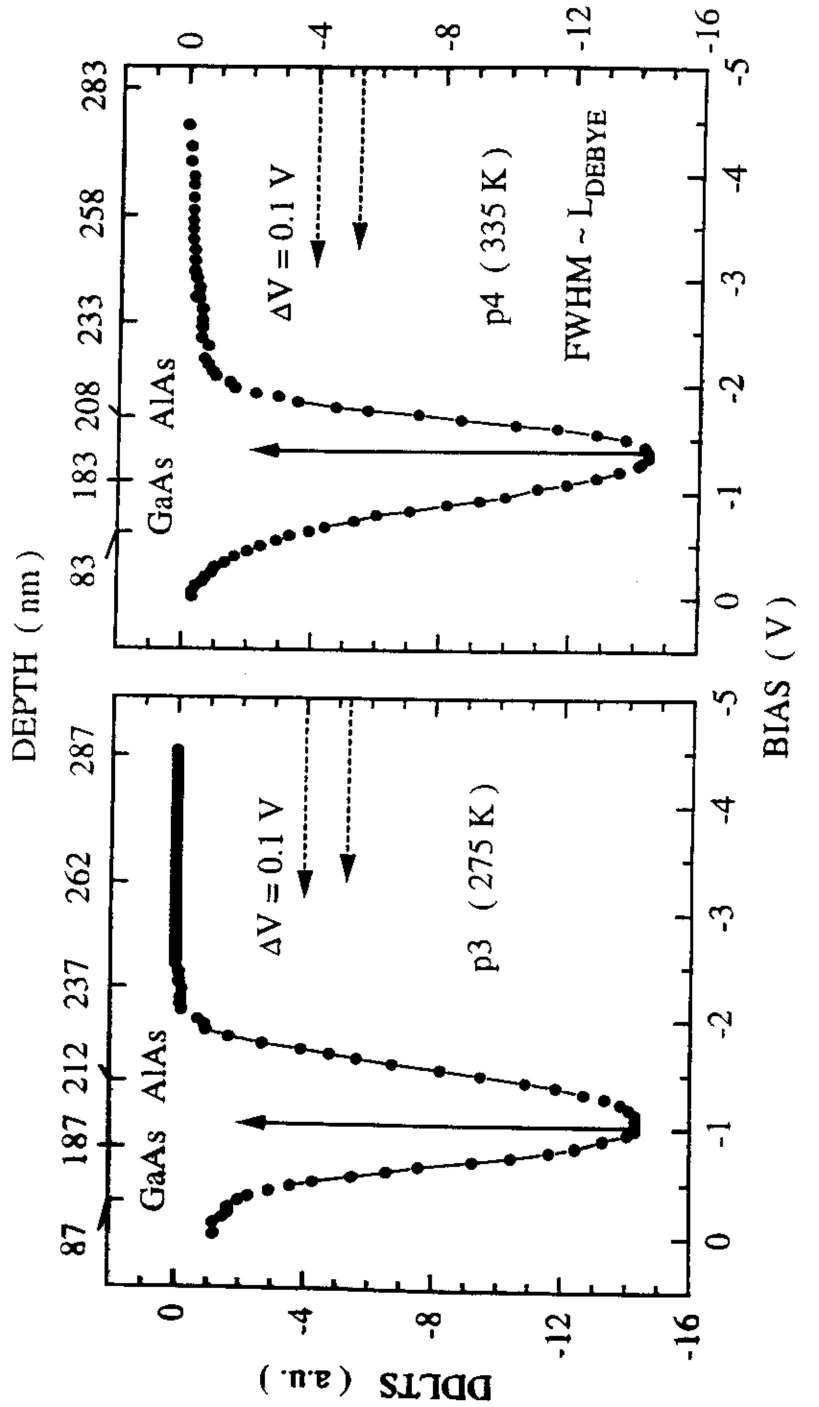

CONCENTRATION OF ISOLATED ARSENIC VACANCIES AT THE GaAs/$Al_xGa_{1-x}As$ INTERFACE

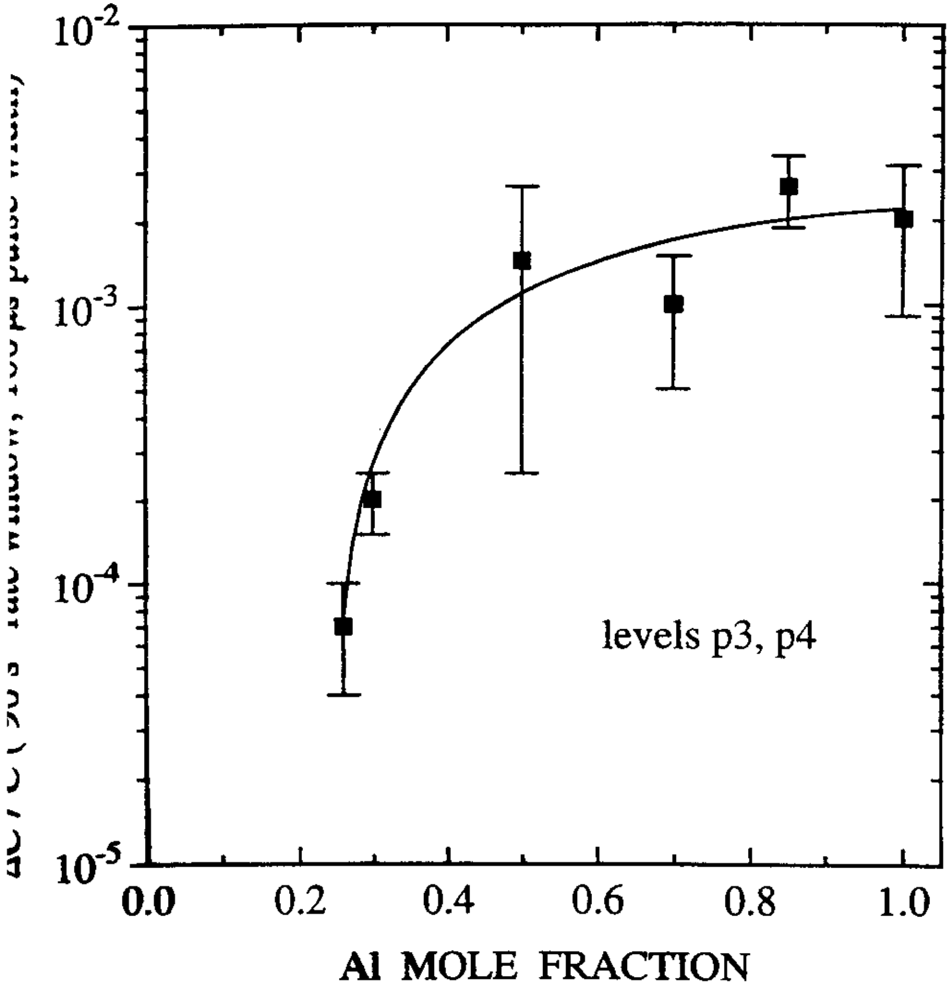

CORRESPONDENCE of p and E levels

p levels at inverted interface	levels in irradiated $Al_xGa_{1-x}As$	Origin	chemical shift exp. (eV)	theor.
p2	DX	$Si_{Ga,Al}$		
p3	E1	V_{As}	0.33	0.37*
p4	E2	V_{As}	0.33	0.37*
p5	E3	V_{As}-As_i	0.29	0.23-0.29#
p6	E4	V_{As}-$As_{Ga,Al}$	0.20	0.23#

* P.J. Lin-Chung and T.L. Reinecke, Phys. Rev. B 27, 1101 (1983)
\# C.W. Myles and O.F. Sankey, Phys. Rev. B 29, 6810 (1984)

SUMMARY DLTS

- **MBE**-grown $Al_xGa_{1-x}As$ **layers** are nearly **defect-free** (apart from the DX center).
- **Intrinsic defects accumulate** on the $Al_xGa_{1-x}As$ side of the inverted (GaAs on $Al_xGa_{1-x}As$) interface, but not at the normal interface.
- **Isolated arsenic vacancies** are formed predominantly near Al atoms and **above a composition threshold** of $x = 0.25$.
- Levels p3 and p4 originating from **the arsenic vacancy V_{As}** are always dominant near the inverted interface despite the **As stable growth conditions**.
- The intrinsic deep levels p3 - p6 are probably connected with an **intrinsic defect configuration at the $Al_xGa_{1-x}As$ surface** during growth.

Single Quantum Well

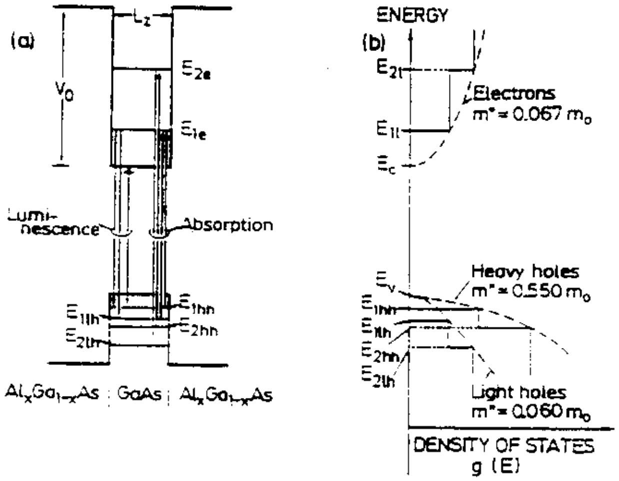

(a) Schematic illustration of electron-hole transitions for emission or absorption of light in a GaAs quantum well; (b) comparison of energy dependence of density of states g(E) in bulk (dotted line) and in a quantum well (solid line).

$$E_n = \frac{\hbar^2 \cdot n^2 \cdot \pi^2}{2m_e^* \cdot L_z^2}$$

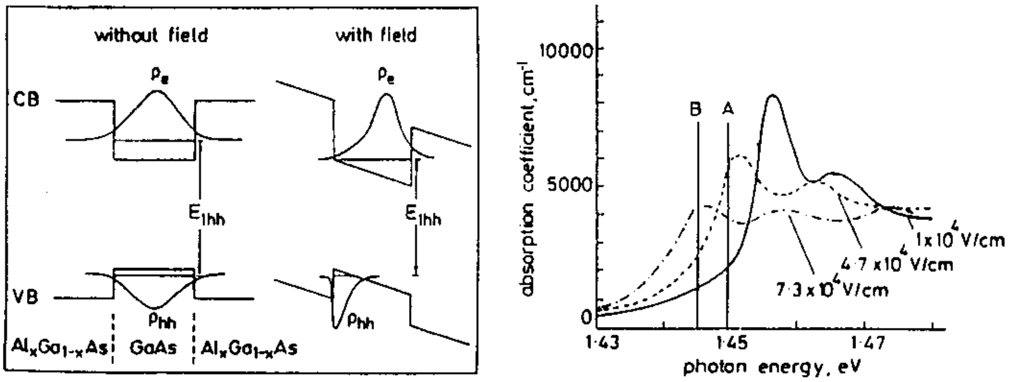

(a) Schematic illustration of the effect of an electric field applied normal to the interfaces on the energy bands and wavefunctions of a quantum well; (b) variation of room-temperature absorption features with electric field.

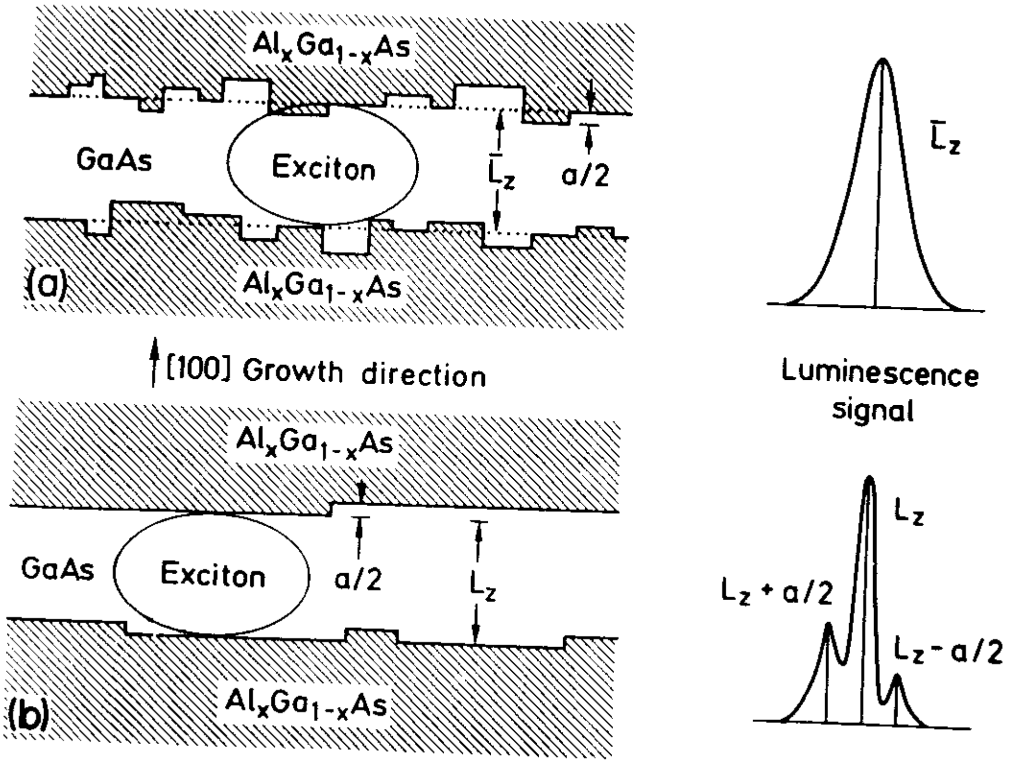

$$\Delta E \simeq \frac{\Delta L_z}{L_z^3}$$

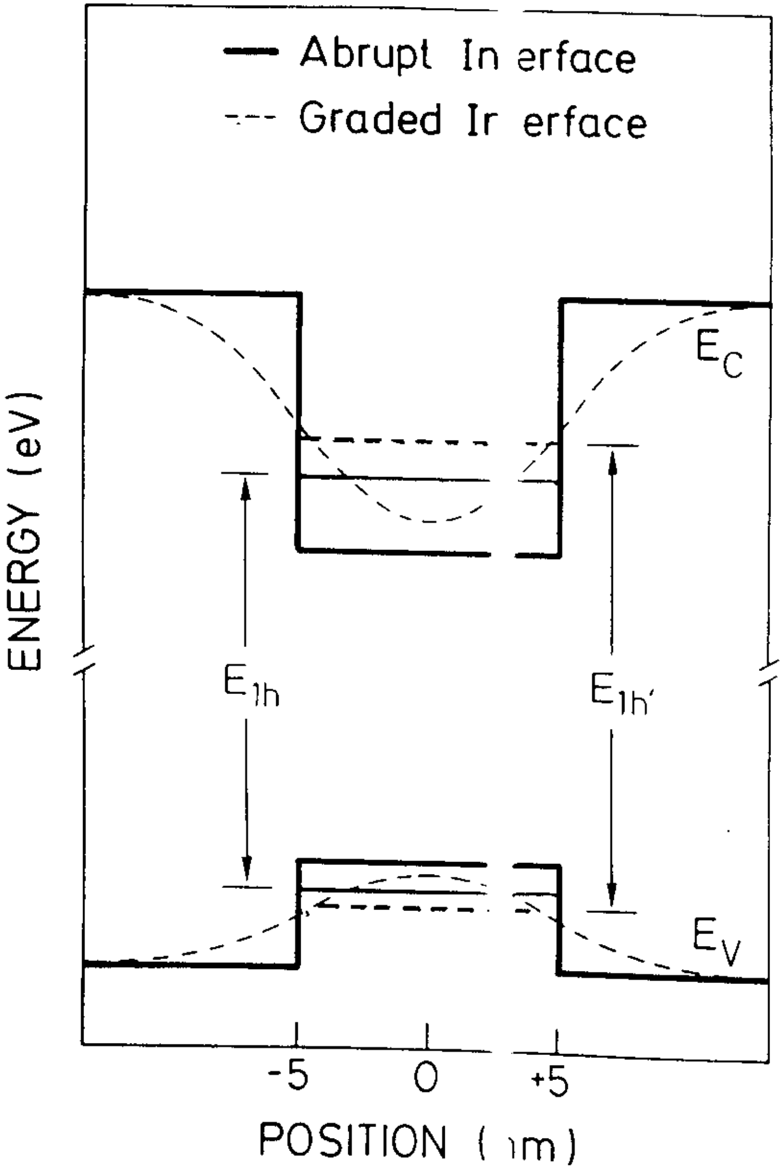

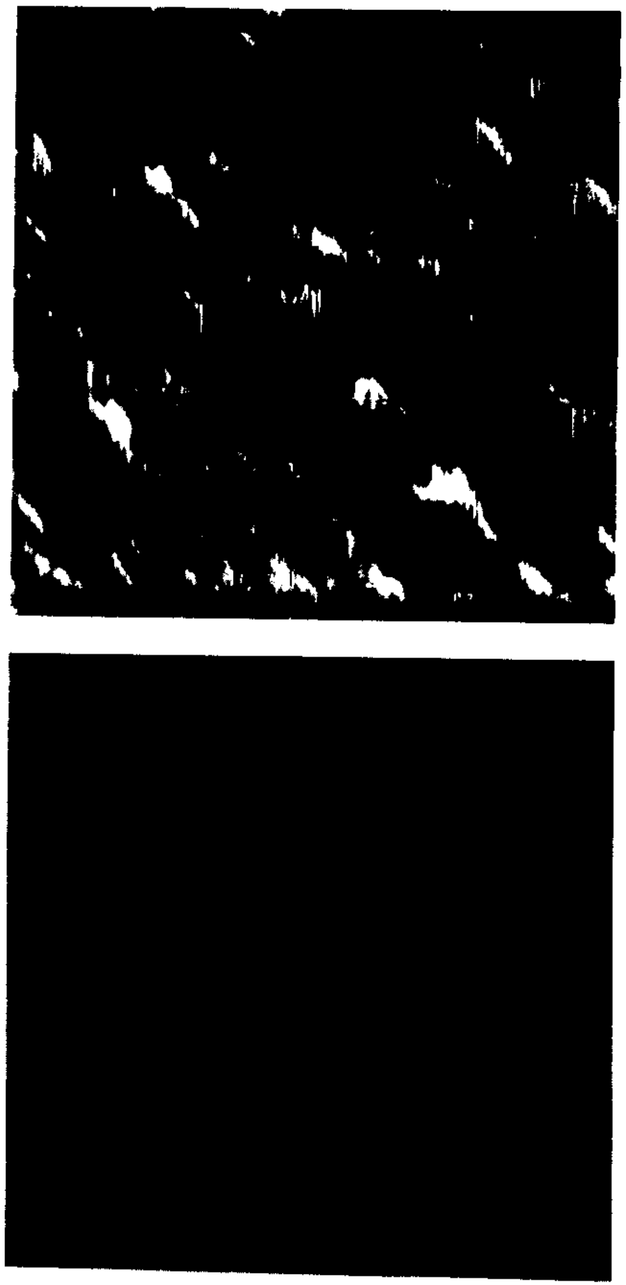

AFM images (3 µm x 3 µm) of the GaAs cap layer surface of QWs with SPSL-barriers grown under ***step flow*** conditions at T_s= 610°C.

As$_4$-to-Ga BEP-ratio = 10 (left) weak (3 x 1) surface reconstruction, miscut = 0.05°
As$_4$-to-Ga BEP-ratio = 30 (right) (2 x 4) surface reconstruction, miscut = 0.02°

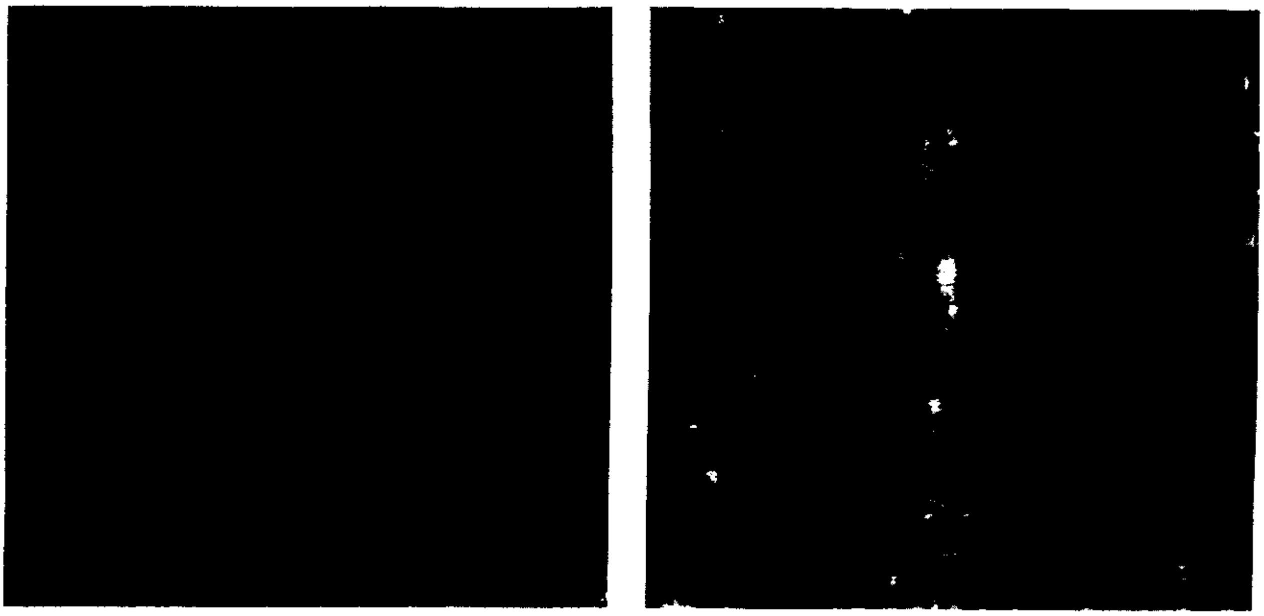

AFM images (3 µm x 3 µm) of the GaAs cap layer surfaces of QWs with SPSL-barriers grown under ***step flow*** (left) and ***two-dimensional nucleation*** (right) conditions.
left: T_s = 640°C; weak (3 x 1) surface reconstruction; As_4/Ga BEP = 10; miscut=0.02°
right: T_s = 550°C; (2 x 4) surface reconstruction; As_4/Ga BEP = 10; miscut=0.02°

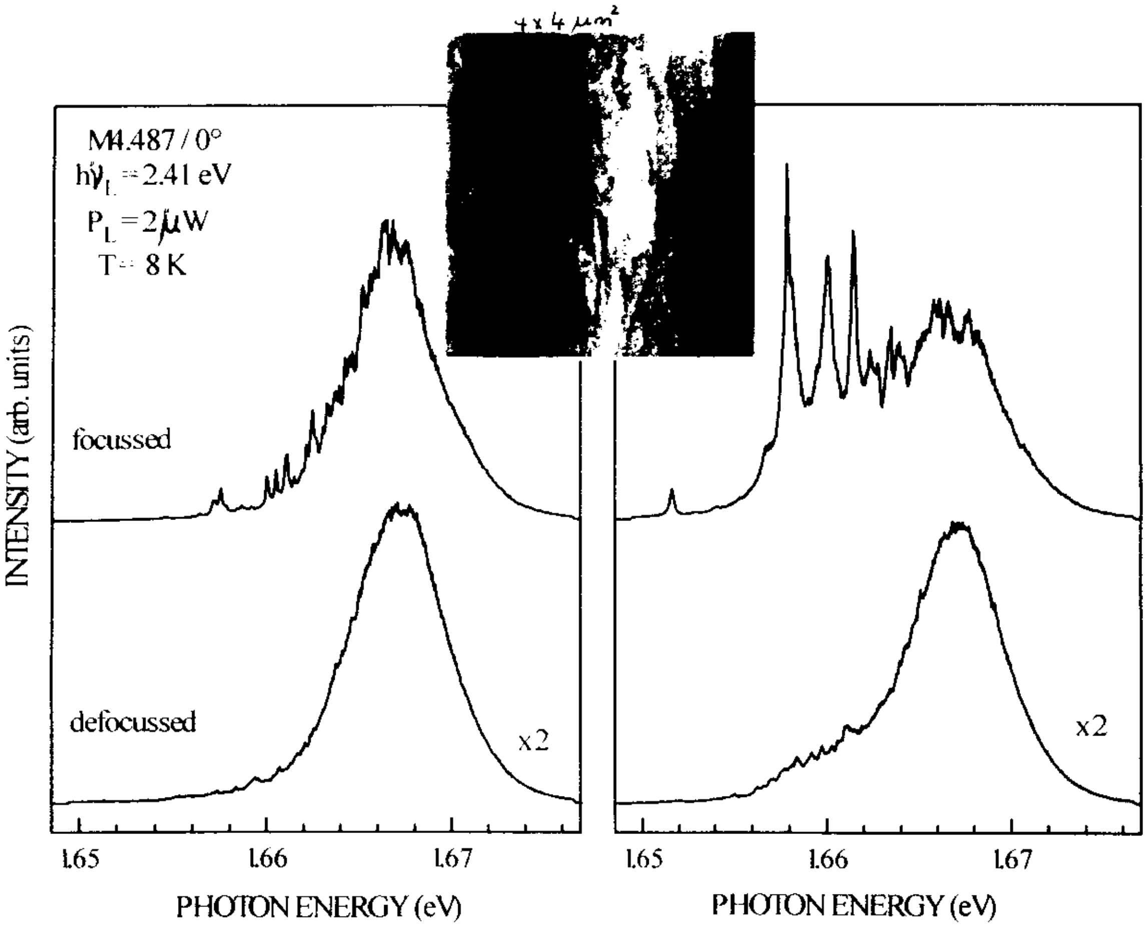

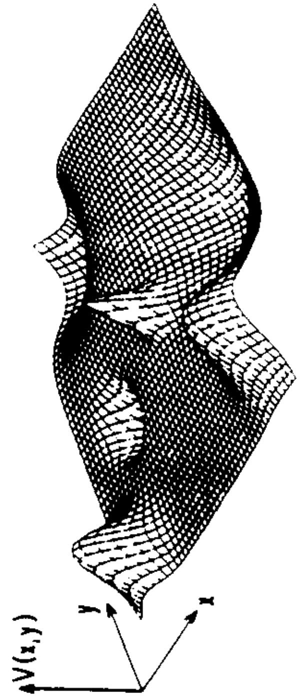

Effective in - plane potential seen by an electron moving in a quantum well with rough interfaces

G. Bastard, R. Ferreira, NATO ASI Series 3 High Tech. Vol. 3

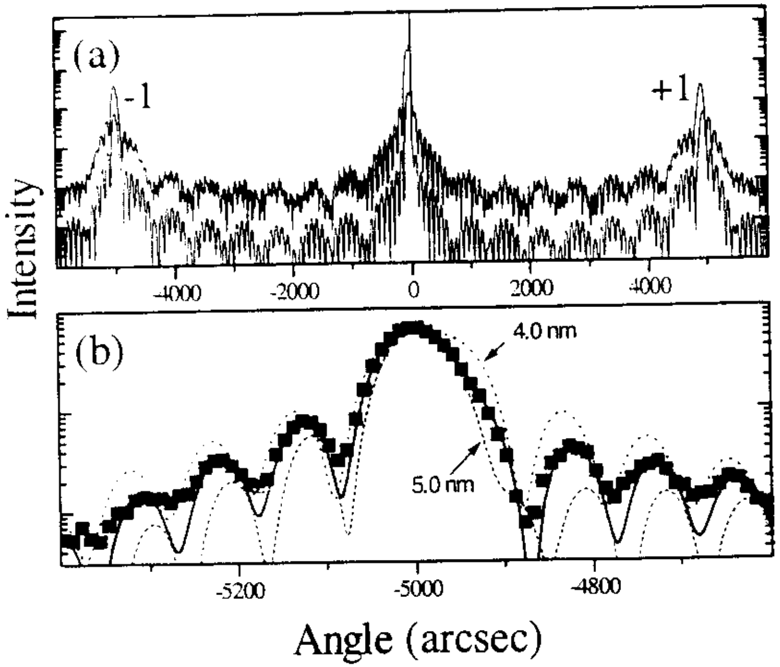

Fig.1. Typical diffractometer curve near the (002) reflection: (a) Comparison of the experimental curve (upper line) with the calculation in dynamical approximation (dotted line below). Clearly pronounced interference fringes are visible. (b) Evaluation of these interference fringes (squares) near the superlattice satellite (-1) for the determination of the average thickness of the quantum well. Calculation for three thicknesses (4.0 nm dotted line, 4.5nm straight line, 5.0 nm dashed line) of the quantum well are presented.

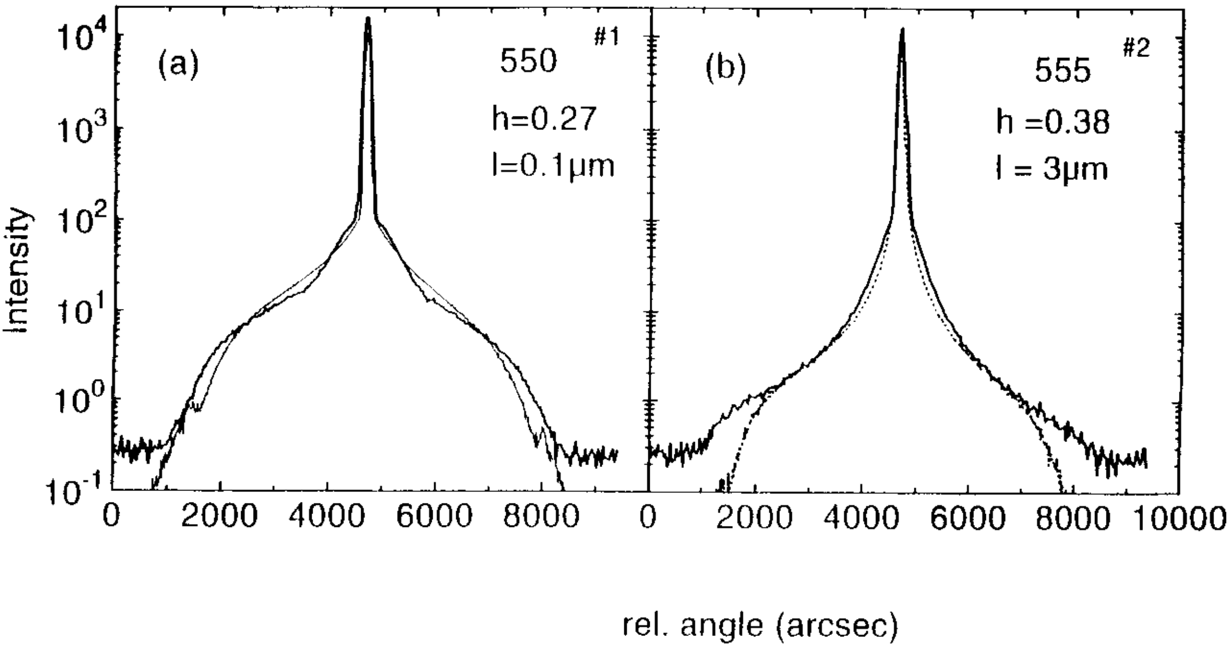

$$C_{j,j'}(x) = [\sigma_j \sigma_{j'} \delta_{j,j'} + \sigma'_j \sigma'_{j'}] \exp\left\{-\left(\frac{x}{\xi}\right)^{2h}\right\}$$

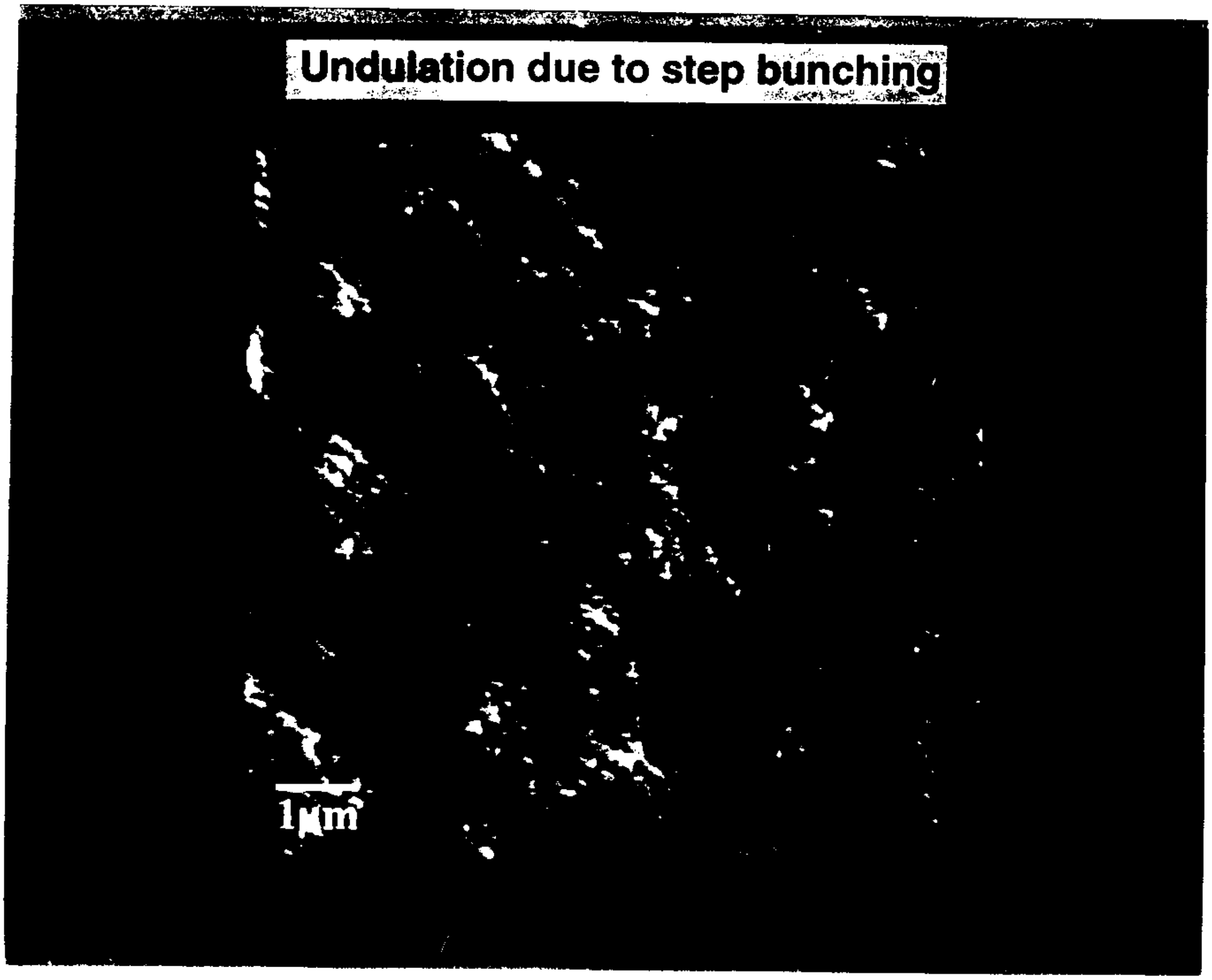
Undulation due to step bunching

PL-Intensities and internal quantum efficiencies at RT-InGaAs/AlGaAs-QW on GaAs of different orientations

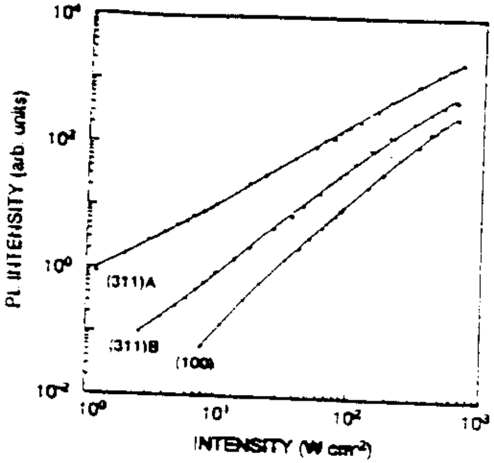

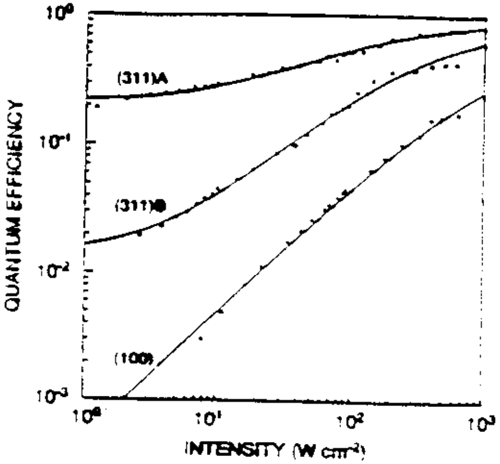

Parameter	(100)	(311)B	(311)A
Radiative lifetime τ_r[a]			
Steady state	≥3.0 μs	≥0.6 μs	80±24 ns
Transient	...	...	91±40 ns
Nonradiative lifetime τ_{nr} (ns)[a]			
Steady state	3.2±0.9	7.6±1.1	19±3
Transient	2.0±1.7	3.4±1.6	17±7
Hole density p_0 (10^{15} cm^{-3})[b]			
$In_{0.1}Ga_{0.9}As$	0.8	0.6	1.6
$Al_{0.33}Ga_{0.67}As$	SI	SI	6.1
Mobility μ (cm^2/V s)[b]			
In $In_{0.1}Ga_{0.9}As$	261	212	269
In $Al_{0.33}Ga_{0.67}As$	SI	SI	139

[a] Obtained as best-fitting parameters for steady state and transient conditions. Error margins represent the confidence intervals of the fits.

[b] As obtained by Hall measurements on thick (~8 μm) layers and corrected for depletion zones. SI indicates high resistivity.

1886 Appl. Phys. Lett., Vol. 67, No. 13, 25 September 1995

Brandt et al.